

## **General Disclaimer**

### **One or more of the Following Statements may affect this Document**

- This document has been reproduced from the best copy furnished by the organizational source. It is being released in the interest of making available as much information as possible.
- This document may contain data, which exceeds the sheet parameters. It was furnished in this condition by the organizational source and is the best copy available.
- This document may contain tone-on-tone or color graphs, charts and/or pictures, which have been reproduced in black and white.
- This document is paginated as submitted by the original source.
- Portions of this document are not fully legible due to the historical nature of some of the material. However, it is the best reproduction available from the original submission.

U  
A

UNITED AIRCRAFT CORPORATION

# United Aircraft Research Laboratories

EAST HARTFORD, CONNECTICUT



|                               |                         |                         |
|-------------------------------|-------------------------|-------------------------|
| FACILITY FORM 602             | <u>N71-38237</u>        | _____                   |
|                               | (ACCESSION NUMBER)      | (THRU)                  |
|                               | <u>49</u>               | <u>63</u> <del>70</del> |
|                               | (PAGES)                 | (CODE)                  |
| <u>CR-123187</u>              | <u>22</u> <del>23</del> | _____                   |
| (NASA CR OR TMX OR AD NUMBER) | (CATEGORY)              |                         |

# United Aircraft Research Laboratories



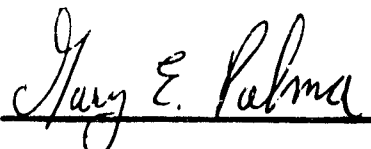
EAST HARTFORD, CONNECTICUT 06108

K-990929-2

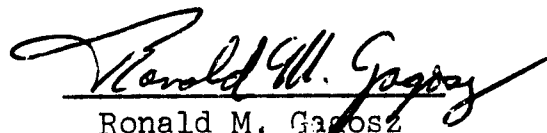
Effect of 1.5 Mev Electron Irradiation  
on the Transmission of Optical Materials

NASA Contract No. BNPC-70

REPORTED BY

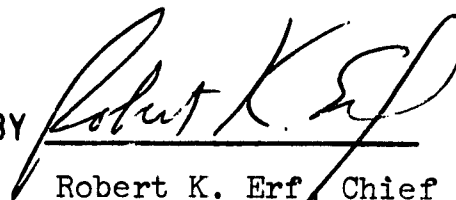


Gary E. Palma



Ronald M. Gagosz

APPROVED BY



Robert K. Erf, Chief  
Optics and Acoustics

DATE September 1971

NO. OF PAGES 49

COPY NO. 26

FOREWORD

An exploratory experimental and theoretical investigation of gaseous nuclear rocket technology is being conducted by the United Aircraft Research Laboratories under Contract SNPC-70 with the joint AEC-NASA Space Nuclear Systems Office. The Technical Supervisor of the Contract for NASA was Captain C. E. Franklin (USAF) for the first portion of the contract performance period and was Dr. Karlheinz Thom for the last portion of the contract performance period. Results obtained during the period September 16, 1970 and September 15, 1971 are described in the following seven reports (including the present report) which comprise the required second Interim Summary Technical Report under the Contract:

1. Roman, W. C. and J. F. Jaminet: Experimental Investigations to Simulate the Thermal Environment and Fuel Region in Nuclear Light Bulb Reactors Using an R-F Radiant Energy Source. United Aircraft Research Laboratories Report K-910900-7, September 1971.
2. Klein, J. F.: Experiments to Simulate Heating of the Propellant in a Nuclear Light Bulb Engine Using Thermal Radiation from a D-C Arc Radiant Energy Source. United Aircraft Research Laboratories Report K-910900-8, September 1971.
3. Bauer, H. E.: Initial Experiments to Investigate Condensation of Flowing Metal-Vapor/Heated-Gas Mixtures in a Duct. United Aircraft Research Laboratories Report K-910900-9, September 1971.
4. Rodgers, R. J., T. S. Latham and H. E. Bauer: Analytical Studies of Nuclear Light Bulb Engine Radiant Heat Transfer and Performance Characteristics. United Aircraft Research Laboratories Report K-910900-10, September 1971.
5. Latham, T. S. and H. E. Bauer: Analytical Design Studies of In-Reactor Tests of a Nuclear Light Bulb Unit Cell. United Aircraft Research Laboratories Report K-910900-11, September 1971.
6. Krascella, N. L.: Spectral Absorption Coefficients of Helium and Neon Buffer Gases and Nitric Oxide-Oxygen Seed Gas Mixture. United Aircraft Research Laboratories Report K-910904-2, September 1971.
7. Palma, G. E. and R. M. Gagosz: Effect of 1.5 Mev Electron Irradiation on the Transmission of Optical Materials. United Aircraft Research Laboratories Report K-990929-2, September 1971. (present report)

ATS-66776

X71-82441

ATS-26774

Report K-990929-2

Effect of 1.5 Mev Electron Irradiation  
on the Transmission of Optical Materials

TABLE OF CONTENTS

|   | <u>Page</u> |
|---|-------------|
| SUMMARY . . . . .   | 1           |
| RESULTS . . . . .   | 2           |
| INTRODUCTION. . . . .   | 4           |
| DESCRIPTION OF EQUIPMENT AND EXPERIMENTAL TECHNIQUE . . . . . | 7           |
| Dynamitron Electron Accelerator . . . . .                     | 7           |
| LINAC Electron Accelerator. . . . .                           | 7           |
| Optical and Electronic System . . . . .                       | 8           |
| Specimen Configuration and Ionizing Dose Rate . . . . .       | 9           |
| EXPERIMENTAL RESULTS. . . . .                                 | 10          |
| Fused Silica Studies. . . . .                                 | 10          |
| Aluminum Oxide Studies - Radiation Annealing. . . . .         | 13          |
| Fluoride Studies - Electron Irradiation . . . . .             | 14          |
| Beryllium Oxide Studies - Electron Irradiation. . . . .       | 15          |
| DISCUSSION OF RESULTS . . . . .                               | 17          |
| REFERENCES. . . . .   | 19          |
| LIST OF SYMBOLS . . . . .                                     | 21          |
| TABLES. . . . .   | 22          |
| FIGURES . . . . .   | 24          |

Report K-990929-2

Effect of 1.5 Mev Electron Irradiation  
on the Transmission of Optical Materials

SUMMARY

A program of experiments was conducted to measure the optical transmission of several transparent materials before, during, and immediately after 1.5 Mev electron irradiation. These experiments were conducted at the Space Radiation Effects Laboratory of the NASA Langley Research Center using a Dynamitron electron accelerator as a source of 1.5 Mev electrons. A preliminary experiment was also conducted to evaluate the feasibility of using the Langley pulsed LINAC electron accelerator as a source of higher energy electrons (3-10 Mev) in future experiments. The Dynamitron experiments included a comparison of irradiation-induced optical absorption in three commercial grades of high-purity fused silica. It was found that the behavior of Corning 7940, Amersil, and Spectrosil high-purity grades of fused silica were similar with regard to the generation, annealing, and optical bleaching of the irradiation-induced optical absorption in the wavelength interval 2000 to 3000 Å. In addition, measurements of the optical transmission of single crystal specimens of aluminum oxide, magnesium fluoride, barium fluoride, lithium fluoride, and beryllium oxide were made during 1.5 Mev electron irradiation in the wavelength interval 2000 to 3000 Å.

## RESULTS

1. Measurements of the optical transmission of Amersil and Spectrosil fused silica before, during, and after 1.5 Mev electron irradiation indicate that:

- a. The spectral shape of the irradiation-induced absorption band centered at a wavelength of 2150 Å does not differ significantly in either material from that measured in Corning 7940 fused silica.
- b. The growth of the induced absorption coefficient at a wavelength of 2150 Å during ambient-temperature irradiation is linear, with an approximate slope of  $0.03 \text{ cm}^{-1}/\text{Mrad}$ , as compared with a range of values of 0.039 to  $0.073 \text{ cm}^{-1}/\text{Mrad}$  for Corning 7940 fused silica obtained previously (Ref. 10).
- c. Reactor irradiation-induced optical absorption can be removed, as in Corning 7940 fused silica, by radiation annealing with 1.5 Mev electrons.
- d. The annealing time constant for isothermal annealing of a reactor-irradiated Amersil specimen at  $600^{\circ}\text{C}$  is 170 sec which is in general agreement with post-irradiation measurements on Corning 7940 fused silica (Ref. 6).
- e. The value of the optical bleaching constant for a reactor irradiated Spectrosil specimen is approximately  $0.09 \text{ watts}^{-1} \cdot \text{cm}^2 \cdot \text{sec}^{-1}$ .

2. Measurement of the optical transmission of a Corning 7940 fused silica specimen after ambient-temperature 7 Mev electron irradiation (LINAC electron accelerator) indicates that the growth rate and spectral shape of the 2150 Å absorption band are not appreciably different from those resulting from 1.5 Mev electron irradiation.

3. Measurement of the optical transmission of a previously reactor-irradiated aluminum oxide specimen during 1.5 Mev electron irradiation indicates that the reactor-induced 2050 Å absorption band, which anneals at a temperature of 500 C in the absence of irradiation, can be removed by radiation annealing with 1.5 Mev electrons at a temperature of 60 C.

4. Measurements of the optical transmission of single crystal specimens of magnesium fluoride, barium fluoride, and lithium fluoride during 1.5 Mev electron irradiation indicates that each of these materials develops broad

K990929-2

optical absorption bands in the wavelength interval 2000-3000 Å during electron irradiation. The growth rates are at least an order of magnitude higher than those measured in fused silica.

5. Preliminary measurements of the optical transmission of BeO during 1.5 Mev electron irradiation indicates a steady-state absorption coefficient at 2500 Å of  $0.8 \text{ cm}^{-1}$  at an ionizing dose rate of 3.5 Mrad/sec and a specimen temperature of  $360^\circ\text{C}$ .



## INTRODUCTION

The Research Laboratories of United Aircraft Corporation have been conducting an extensive program to determine the effects of nuclear radiation on the optical transmission of transparent materials under NASA Contracts NASw-768, NASw-847, and SNPC-70, and under Corporate sponsorship. The purpose of this program has been to determine the level of irradiation-induced optical absorption to be expected in the transparent wall of a full-scale nuclear light bulb engine during normal operation. The material studied most extensively throughout these programs has been Corning 7940 fused silica. Fused silica has good optical transmission, good thermal and structural properties, and is relatively easy to fabricate. In addition, irradiation-induced absorption bands at visible wavelengths, which are related to impurities, do not develop appreciably in high-purity grades of fused silica such as Corning 7940. The irradiation-induced absorption bands that are observed after exposure to nuclear radiation are centered at the ultraviolet wavelengths of approximately 2150 Å and 1650 Å, with additional structure sometimes observed near 2700 Å (Ref. 1 through 5).

Previous experimental programs have consisted of four distinct sets of experiments which included:

1. Post-irradiation optical transmission measurements in which the reactor irradiation simulated the full-scale engine dose (Ref. 6);
2. In-situ optical transmission measurements in a pulsed reactor which simulated the full-scale engine dose rate (Refs. 7 and 8);
3. In-situ optical transmission measurements in a steady-state reactor which simulated the full-scale engine dose (Ref. 9); and
4. In-situ optical transmission measurements in an electron accelerator which simulated the ionizing dose and dose rate of the full-scale engine (Ref. 10).

These previous investigations have been restricted almost exclusively to the study of Corning 7940 fused silica at wavelengths longer than 2000 Å. It was found that the most prominent absorption band (2150 Å) was generated by ionizing radiation and that the growth rate at a given ionizing dose rate was independent of the type of radiation (i.e. gamma ray, reactor, or electron). Thus, a radiation source with an ionizing dose rate comparable to the full-scale engine ( $\sim 5$  Mrad/sec) could provide a simulation of the radiation effects expected in a transparent wall of high purity fused silica. These high ionizing dose rates were obtained during the FY 1969 and FY 1970 programs with a 1.5

Mev Dynamitron electron accelerator. In particular, accurate measurements of the optical transmission of fused silica were made at ambient and elevated temperatures during 1.5 Mev electron irradiation in the FY 1970 program (Ref. 10). Extensive measurements of the steady-state irradiation-induced absorption coefficient at 2150 Å were made over a wide range of ionizing dose rates (.02-5 Mrad/sec) and specimen temperatures (100-500°C). It was found that, at constant ionizing dose rate, the induced absorption coefficient decreased with increasing specimen temperature due to the corresponding increase in the thermal annealing rate. However, at constant temperature, the absorption coefficient increased with increasing ionizing dose rate up to a dose rate of 0.4 Mrad/sec. Above an ionizing dose rate of 0.4 Mrad/sec the induced absorption coefficient decreased with further increases in dose rate. This variation of the steady-state induced absorption coefficient with dose rate could be interpreted if it was assumed that the annealing rate increased rapidly with dose rate, a phenomena that is referred to as radiation annealing. This interpretation was verified by removing reactor irradiation-induced absorption with 1.5 Mev electron irradiation at temperatures at which the thermal annealing rate is known to be negligible. In addition, measurements of the rate of removal of induced absorption by bleaching with ultraviolet light were made at low light intensities. Extrapolation of these results to the light intensity expected in the full-scale engine indicated that optical bleaching may reduce the level of irradiation-induced absorption by an order of magnitude. Based on these results, the expected additional heat load, due to radiation-induced absorption in the transparent wall, was found to be negligible for the case of high purity Corning 7940 fused silica.

High purity fused silica has an intrinsic ultraviolet cutoff wavelength of approximately 1600 Å, beyond which it is highly opaque. A transparent material with a lower ultraviolet cutoff could transmit a greater fraction of the radiant energy emitted by the fuel region of the nuclear light bulb engine and could result in a more efficient engine. In particular, a transparent wall material with a significantly lower ultraviolet cutoff would be of interest in a higher performance version of the nuclear light bulb engine whose radiating temperature would be higher than the nominal value of 15,000°R. Any such promising candidate material should also have thermal and structural properties comparable to or exceeding those of fused silica and must also remain relatively transparent during nuclear irradiation.

The present experimental program was conducted in order to determine if any other available transparent materials could offer improved performance over Corning 7940 fused silica as the transparent wall material in the nuclear light bulb engine. The new materials studied included high purity Amersil and Spectrosil fused silica, and single crystal specimens of aluminum oxide, magnesium fluoride, barium fluoride, lithium fluoride, and beryllium oxide. The optical transmission range, the melting point, and the thermal conductivity

of these materials are presented in Table I. It can be seen that all of the new materials have a broader optical transmission range in the absence of irradiation than fused silica. In addition, aluminum oxide and beryllium oxide have higher melting points and higher thermal conductivity than fused silica, and have better structural integrity than the fluoride materials.

The experiments described in this report consisted primarily of in-situ measurements of the optical transmission of the above mentioned transparent materials during 1.5 Mev electron irradiation in the wavelength interval 2000-3000 Å. The motivation, design, procedure, and results for each of the experiments are described in the following sections. Also included is a description of the optical system modifications made during the present program which will permit optical transmission measurements at wavelengths shorter than 2000 Å in future experiments.

## DESCRIPTION OF EQUIPMENT AND EXPERIMENTAL TECHNIQUE

The electron irradiation experiments were conducted at the Space Radiation Effects Laboratory of the NASA Langley Research Center, Hampton, Virginia, using the Dynamitron electron accelerator as a source of 1.5 Mev electrons. The SREL pulsed LINAC electron accelerator was also used in a single 7 Mev electron irradiation experiment. The system used to make the in-situ measurements of optical transmission during the electron irradiation is similar to that used in the FY 1970 program and is described in Ref. 10. Certain modifications were made to this system to permit measurements at wavelengths as short as 1550 Å, but, to date, this added capability has not been demonstrated during electron irradiation tests.

## Dynamitron Electron Accelerator

The Dynamitron electron accelerator is a linear beam device that provides a continuous 1-cm-diameter electron beam through a water cooled, thin (0.001-in.) titanium window. In order to obtain an electron kinetic energy of 1.5 Mev at the output of the beam port, it is necessary to run at a beam energy of 1.6 Mev to correct for the 0.1 Mev energy loss due to the titanium window. Upon passing through the titanium window, the electron beam is also scattered resulting in a loss of collimation. In order to compensate for this effect, 1-cm-diameter apertures were used at the output beam port of the accelerator and at the input of the specimen furnace assembly to provide the necessary collimation. With this configuration, a maximum current density of 100 microamps/cm<sup>2</sup> in a well collimated 1-cm-diameter beam could be obtained at the location of the specimen, 1.5 in. from the beam port.

## LINAC Electron Accelerator

The LINAC electron accelerator is a repetitively pulsed device that has an electron energy range of 3 to 10 Mev. The maximum average current density is 200 microamps/cm<sup>2</sup> in a 1-cm-diameter beam at the accelerator exit port. The pulse width and repetition rate are variable over the ranges 0.01 - 1 µsec and 1-300 pps respectively. The geometrical configuration is almost identical to that of the Dynamitron accelerator.

## Optical and Electronic System

Figure 1 is a combined optical and electronic schematic that illustrates, in functional form, the important experimental components with their respective locations: for measurements at wavelengths longer than 2000 Å, this system is identical to that described in detail in Ref. 10. However, certain modifications were required to extend the lower wavelength limit to 1550 Å: the fused silica window on the hydrogen lamp was replaced with a LiF window; the fused silica prism in the monochromator was replaced with a reflecting grating; and all the reflecting optics were re-aluminized and overcoated with  $MgF_2$  in order to enhance reflectivity at the shorter wavelengths. The ASCOP 543-1014 photomultiplier is sensitive to wavelengths as short as 1450 Å and is considered adequate for this application.

In addition to these optical component modifications, it is necessary to reduce the concentration of oxygen and water vapor to an acceptable level in order to eliminate the loss of signal due to the strong optical absorption of these gases at wavelengths shorter than 1800 Å. The standard technique is to evacuate the entire optical system; vacuum ultraviolet spectroscopy is the term usually used to describe measurements made in this spectral region. However, evacuation of the present system would have required the replacement of many of the existing components, including the furnace assembly, and would have been extremely difficult to effect because of the size of the chamber and the required interface with the electron accelerator. An alternate technique, chosen for these experiments and shown in Fig. 1, is to purge the system with high purity nitrogen or argon. The required purity can be calculated from absorption cross section data for oxygen and water vapor as shown in Figs. 2 and 3 (Ref. 11). At atmospheric pressure, the oxygen and water vapor content must be kept below approximately 50 parts per million in order to obtain adequate transmission over a path length of 1 meter, the approximate distance in the experimental system. Of additional interest is the fact that if oxygen is present, the ultraviolet radiation from the hydrogen lamp will generate a certain amount of ozone. While ozone does not absorb appreciably in the wavelength interval 1550-2000 Å, it does have a strong absorption band at 2500 Å (shown in Fig. 4) and thus, can be used to monitor the removal of oxygen by the purge gas. The experimental system, as described above, was operated in a laboratory environment using both nitrogen and argon as purge gases, and adequate optical signal strength was obtained in the wavelength interval 1550-2000 Å. However, when the system was set up on site, and interfaced with the Dynamitron accelerator, it was not possible to obtain adequate signal strength below a wavelength of 2000 Å. The cause of this difficulty has not been fully resolved as yet, but it is felt that the loss of signal was probably the result of either gas impurities, degradation of the optical coatings, and/or chemical attack on the LiF window.

### Specimen Configuration and Ionizing Dose Rate

The specimen configuration used was the same as in the FY 1970 program in which the specimen is mounted in the furnace assembly at an angle of 65 deg with respect to the electron beam axis and at an angle of 25 deg with respect to the optical beam axis. In this way a large interaction region is provided between the incident optical beam and the irradiated region (Ref. 10).

The ionizing dose rate generated in a material by a given electron current density depends upon the incident electron energy  $E$ , and the atomic number  $Z$  and atomic weight  $A$  of the target material. The variation of the energy loss per unit length, or stopping power, with incident electron kinetic energy for  $Z = 5$  and  $Z = 25$  is presented in Fig. 5. The curves have been normalized to a factor proportional to  $Z/A$ , which is approximately constant for low  $Z$  materials. Examination of Fig. 5 indicates that the stopping power does not vary appreciably with atomic number or electron energy in the range  $1 < E < 10$  Mev. The ionizing dose rate is approximately proportional to the product of the stopping power and the current density:

$$\dot{D} \approx 0.1 \frac{J \frac{dE}{dx}}{\rho} \quad (\text{Mrad/sec}) \quad (1)$$

where:

$J$  = current density (microamp/cm<sup>2</sup>)

$\frac{dE}{dx}$  = stopping power (Mev/cm)

$\rho$  = target material density (gm/cm<sup>3</sup>)

Since the stopping power is proportional to  $\rho$ , and does not vary appreciably with  $Z$ , the ionizing dose rate at a given current density should be approximately independent of the target material. In order to accurately calculate the ionizing dose rate from the stopping power, it is necessary to include a correction for the divergence of the electron beam as it passes through the medium (Ref. 12). The results of the calculation of the ratio of the ionizing dose rate  $\dot{D}$  to the current density  $J$  at an electron energy of 1.5 Mev are presented in Table II for the transparent materials of interest. As expected, the ratio does not vary appreciably among these materials.

## EXPERIMENTAL RESULTS

The experimental results are expressed as induced absorption coefficients which are calculated from the chart recorder data using the following equation:

$$\alpha(\lambda) = \frac{1}{\ell} \ln \left[ \frac{I(\lambda, T, \dot{D}, t)}{I_0(\lambda)} \right] \quad (2)$$

where:

- $\alpha(\lambda)$  = irradiation-induced absorption coefficient at the wavelength  $\lambda$  ( $\text{cm}^{-1}$ )
- $\ell$  = optical path length through specimen (cm)
- $I_0(\lambda)$  = chart recorder amplitude prior to irradiation
- $I(\lambda, T, \dot{D}, t)$  = chart recorder amplitude at a time  $t$  after turn-on of electron beam.

## Fused Silica Studies

A total of seven high purity fused silica specimens (three Amersil grade, three Spectrosil grade, and one Corning 7940 UV grade) were investigated in the present program. One each of the Amersil and Spectrosil specimens were used to study the growth of induced absorption during 1.5 Mev electron irradiation. The remaining two Amersil and Spectrosil specimens had been previously reactor irradiated to a fast neutron dose of  $10^{17}/\text{cm}^2$  in the Union Carbide Research Reactor, in Tuxedo, N.Y.; these were used to study the effect of radiation annealing, thermal annealing and optical bleaching. The Corning 7940 UV grade specimen was used for the preliminary experiments with 7 Mev electron irradiation.

1.5 Mev Electron Irradiation Studies - Amersil and Spectrosil

Measurements of the growth of the induced absorption coefficient at 2150 Å during ambient temperature 1.5 Mev electron irradiation in the previously un-irradiated Amersil (A-1) and Spectrosil (S-1) specimens are shown in Figs. 6 and 7, respectively. At an ionizing dose rate of 0.05 Mrad/sec, the induced absorption increases linearly with ionizing dose in both irradiations with slopes of  $0.03 \text{ cm}^{-1}/\text{Mrad}$  and  $0.025 \text{ cm}^{-1}/\text{Mrad}$  respectively. These values are slightly less than the range of values ( $0.039$  to  $0.073 \text{ cm}^{-1}/\text{Mrad}$ ) that was measured in similar experiments on Corning 7940 fused silica during the FY 1970 program. This difference may be due to the lower ionizing dose rate ( $0.02 \text{ Mrad/sec}$ ) employed in the FY 1970 experiments.

Radiation Annealing Studies - Amersil and Spectrosil

Radiation annealing of reactor-irradiation-induced absorption at 2150 Å in Amersil specimen AN-1 during 1.5 Mev electron irradiation is illustrated in Fig. 8. The initial absorption coefficient of approximately  $18 \text{ cm}^{-1}$  decreases to a value of  $1.3 \text{ cm}^{-1}$  during irradiation at an ionizing dose rate of 0.75 Mrad/sec and a maximum specimen temperature of 220°C. At this specimen temperature the thermal annealing rate in the absence of irradiation would not cause this rapid decrease in absorption. This data thus indicates that radiation annealing is also effective in Amersil fused silica as well as in Corning 7940 fused silica. After an elapsed time of 1150 sec the electron beam was turned off and the absorption coefficient decreased rapidly from  $1.3 \text{ cm}^{-1}$  to  $0.3 \text{ cm}^{-1}$  in approximately 20 sec. This increase in transmission may be the result of a change in signal, not related to optical absorption. Several characteristics of this anomalous change of signal support this conclusion. First, the loss of signal recovers after the electron beam is turned off at a rate that is too rapid to be due to thermal annealing. Second, the anomalous loss of signal was observed at visible wavelengths at which the high purity fused silica remains transparent after prolonged irradiation. Finally, the level of anomalous absorption could be changed by altering the mounting configuration of the specimen and in fact was significantly reduced by using a smaller (1 cm by 1 cm by 1.5 mm) specimen. These factors, and the fact that it has been possible to cause a loss of signal in the optical system by irradiating the specimen with a  $\text{CO}_2$  laser beam which does not generate optical absorption, as described in Ref. 10, indicate that the loss of signal may be due to refractive effects. In particular, if a temperature gradient exists across the face of the specimen, this will result in a gradient in the index of refraction which will give the specimen the characteristics of a lens. The exact shape of the specimen temperature distribution will determine the focal length and aberrations of this equivalent lens. Both the focusing and the aberrations can alter the location and intensity of the focused spot on the entrance slit of the monochromator and can thus cause a change in the intensity transmitted through the slit. For example, an angular deflection of the light beam, as it passes through the specimen, of 0.2 deg would cause a change in position of the focused spot of approximately 2 mm which would move the light beam off the entrance slit of the monochromator and cause a complete loss of signal. In addition, estimates of the temperature gradient and the resulting index of refraction variation across the face of the specimen due to a Gaussian electron beam profile indicate that appreciable defocusing and spherical aberrations could occur during high-dose rate electron irradiation.

After removal of the reactor-irradiation induced absorption by radiation annealing, specimen AN-1 was then re-irradiated at an ionizing dose rate of 0.05 Mrad/sec and at ambient temperature. The subsequent growth of the induced absorption at 2150 Å is shown in Fig. 9. The shape of the growth curve



is not significantly different from that shown in Fig. 6 for the previously unirradiated Amersil specimen A-1, except for a small difference of about  $0.5 \text{ cm}^{-1}$  in the initial portion of the curve, indicating almost complete removal of defects by the radiation annealing treatment.

The results of radiation annealing of reactor-irradiation-induced absorption in Spectrosil specimen SN-1 are shown in Fig. 10. After removing a large fraction of the initial absorption coefficient of  $23 \text{ cm}^{-1}$  at an ionizing dose rate of  $0.75 \text{ Mrad/sec}$  and a specimen temperature of  $200^\circ\text{C}$ , the ionizing dose rate was increased to  $1.5 \text{ Mrad/sec}$  and the specimen temperature raised to  $350^\circ\text{C}$ . The absorption coefficient then decreased to a final value of  $2 \text{ cm}^{-1}$  which decreased rapidly to zero when the electron beam was shut off. As in the previous radiation annealing experiment on Amersil specimen AN-1, the rapid recovery of the transmission after the electron beam is turned off indicates that this fraction of the transmission loss was not due to optical absorption.

The growth of the induced absorption coefficient during subsequent re-irradiation of Spectrosil specimen SN-1 at ambient temperature is shown in Fig. 11. The shape of the initial portion of the growth curve differs from that of previously unirradiated Spectrosil specimen S-1 shown in Fig. 7 by about  $0.6 \text{ cm}^{-1}$  indicating almost complete removal of the defects responsible for the initial absorption coefficient of  $23 \text{ cm}^{-1}$ .

#### Thermal Annealing Studies - Amersil

The results of thermal annealing of reactor-irradiation induced absorption in Amersil specimen AN-2 are shown in Fig. 12. The initial absorption coefficient of  $21 \text{ cm}^{-1}$  begins to decay after the specimen temperature exceeds  $450^\circ\text{C}$ . The specimen temperature was raised to a final value of  $600^\circ\text{C}$  and the absorption was completely removed at this temperature. Measurement of the decay of the absorption coefficient during the constant temperature portion of the anneal indicates a thermal annealing time constant of approximately 170 sec at  $600^\circ\text{C}$  in this material. This is in essential agreement with the results of post-irradiation measurements on Corning 7940 fused silica reported in Ref. 6. The growth of the induced absorption coefficient during subsequent ambient temperature electron irradiation shown in Fig. 13 is characterized by a rapid initial growth, followed by a slower linear growth, indicating that complete removal of defects was not achieved by annealing at  $600^\circ\text{C}$ .

#### Optical Bleaching Studies - Spectrosil

The results of ambient-temperature irradiation with 1.5 Mev electrons, following optical bleaching of reactor-irradiation-induced absorption in Spectrosil specimen SN-2, are shown in Fig. 14. The sample was bleached by

K990929-2

exposure to ultraviolet light with an intensity of 2 mwatt/cm<sup>2</sup> in the 2000 to 2200 Å wavelength region from a BH-6 mercury lamp at ambient temperature for 45 min. During this period the initial absorption coefficient of 16 cm<sup>-1</sup> decreased to 9 cm<sup>-1</sup>. This corresponds to an optical bleaching rate constant of 0.09 watts<sup>-1</sup> - cm<sup>2</sup> - sec<sup>-1</sup>, which is in good agreement with the value of 0.08 watt<sup>-1</sup> - cm<sup>2</sup> - sec<sup>-1</sup> for Corning 7940 fused silica that was reported in Ref. 10.

#### 7 Mev Electron Irradiation Studies - Corning 7940 UV Grade

A preliminary experiment utilizing the LINAC electron accelerator was conducted in which a specimen of Corning 7940 fused silica was irradiated with 7 Mev electrons at an average ionizing dose rate of 0.1 Mrad/sec at ambient temperature to a total dose of 190 Mrad. The spectral absorption in the wavelength interval 2000-3000 Å that was measured after this irradiation is shown in Fig. 15. The location and shape of the absorption band is comparable to that resulting from 1.5 Mev electron irradiation or reactor irradiation. The absorption coefficient of 6.2 cm<sup>-1</sup> at 2150 Å due to the total ionizing dose of 190 Mrad corresponds to a growth rate of approximately 0.033 cm<sup>-1</sup>/Mrad. This is comparable to the growth rate measured during 1.5 Mev electron irradiation and suggests that the growth rate does not vary significantly with electron kinetic energy.

Normalized spectral data of all the irradiation-induced absorption measurements (those due to reactor irradiation, 1.5 Mev electron irradiation, and 7 Mev electron irradiation) made during the present program are plotted in Fig. 16. The solid curve represents an average of the spectra for the Amersil, Spectrosil and Corning specimens irradiated during the present program while the dashed curve is a typical spectrum obtained from previous measurements on Corning 7940 fused silica (Ref. 10).

#### Aluminum Oxide Studies - Radiation Annealing

Measurements of the optical transmission of aluminum oxide during 1.5 Mev electron irradiation conducted during the FY 1970 program indicated that 1.5 Mev electrons are ineffective in generating absorption in this material (Ref. 10). However, reactor irradiation of aluminum oxide results in a strong absorption band centered at 2050 Å which anneals at a temperature of 500 C in the absence of irradiation. Figure 17 shows the results of an experiment in which an aluminum oxide specimen that had been reactor irradiated to a dose of 10<sup>17</sup> n/cm<sup>2</sup> was re-irradiated with 1.5 Mev electrons, resulting in radiation annealing of the absorption band centered at 2050 Å. The initial absorption coefficient was approximately 22.5 cm<sup>-1</sup>, and this absorption coefficient decreased to a steady-state value of 15.5 cm<sup>-1</sup> as a result of electron irradiation

at 0.75 Mrad/sec and 60 deg C. When the dose rate was increased to 1.5 Mrad/sec, and the temperature to 100 deg C, the steady-state absorption coefficient decreased to  $7 \text{ cm}^{-1}$ . A further increase in dose rate and temperature to 3 Mrad/sec and 160 deg C, respectively, resulted in a steady-state absorption coefficient of approximately  $3 \text{ cm}^{-1}$ . This removal of coloration during electron irradiation, although not complete, can be interpreted as radiation annealing since the removal of coloration by pure thermal annealing is ineffective below specimen temperatures of 500 deg C in this material. (Similar results were obtained in the FY 1970 program but were not considered conclusive since the specimen shattered during the high-dose-rate irradiation due to thermal shock.)

### Fluoride Studies - Electron Irradiation

Electron irradiation and optical transmission measurements were made on three different fluoride materials. The latter data was taken over the wavelength interval from 2000 to 3000 Å, with primary attention paid to 2600 Å in  $\text{MgF}_2$  and 2500 Å in  $\text{BaF}_2$  and  $\text{LiF}$ , the expected locations of the peaks of strong irradiation-induced absorption bands in these materials (Ref. 13).

#### Magnesium Fluoride

The results of electron irradiation of a previously un-irradiated single crystal  $\text{MgF}_2$  specimen are shown in Fig. 18. After the electron beam was turned on at 1 microamp/cm<sup>2</sup>, the induced absorption coefficient increased rapidly and saturated at  $20 \text{ cm}^{-1}$ . (The initial rate of coloration at 2600 Å in  $\text{MgF}_2$  is approximately 20 times greater than the corresponding rate of coloration at 2150 Å in fused silica.) The specimen temperature was then raised from 40 deg C to 400 deg C, with the furnace, and the absorption coefficient was observed to decrease above a temperature of 350 deg C, indicating an annealing threshold at this temperature. A further increase in specimen temperature revealed a second annealing process that becomes effective at 600 deg C. However, at 600 deg C and a current density of only 1 microamp/cm<sup>2</sup>, the induced absorption coefficient at 2600 Å was still approximately  $3 \text{ cm}^{-1}$ .

The induced absorption spectrum of  $\text{MgF}_2$  measured in the time interval 1000-1120 sec during this irradiation over the wavelength interval 2000-3000 Å is shown in Fig. 19. The induced absorption band appears to be peaked near 2500 Å and has a width at half-maximum of almost 1000 Å.

#### Barium Fluoride

The results of electron irradiation of a previously un-irradiated single crystal  $\text{BaF}_2$  specimen are shown in Fig. 20. When the electron beam was turned

on at 1 microamp/cm<sup>2</sup>, the induced absorption coefficient increased rapidly to a final value of 3.8 cm<sup>-1</sup>. (The initial growth rate is approximately 20 times greater than the corresponding rate in fused silica.) Further increases in current density to 3 and 5 microamp/cm<sup>2</sup> resulted in steady-state absorption coefficients of 4.1 cm<sup>-1</sup> and 4.9 cm<sup>-1</sup>, respectively. An attempt to raise the specimen temperature with the furnace resulted in fracture of the specimen due to thermal shock.

The induced absorption spectrum of BaF<sub>2</sub> measured in the time interval 700-820 sec during this irradiation over the wavelength interval 2000-3000 Å is shown in Fig. 21. The spectral absorption does not appear to have a simple band structure, and there is indication that the absorption is significant at wavelengths beyond the range of the spectral scan.

#### Lithium Fluoride

The results of electron irradiation of a previously un-irradiated single crystal LiF specimen are shown in Fig. 22. When the electron beam was turned on at an ionizing dose rate of .05 Mrad/sec, the induced absorption coefficient rose rapidly and saturated at a value of 21 cm<sup>-1</sup>. Increasing the temperature to 400°C had no effect on the level of absorption, indicating a very slow annealing rate in this material.

The induced absorption spectrum of LiF measured in the time interval 800-920 sec during this irradiation over the wavelength interval 2000-3000 Å is shown in Fig. 23. The spectral absorption is relatively flat out to a wavelength of 2800 Å, beyond which the transmission begins to increase.

#### Beryllium Oxide Studies - Electron Irradiation

A single crystal specimen of beryllium oxide, 1/2 cm by 1/2 cm by 1 mm, was obtained from North American Autonetics for study in the present program. Since single crystals of good optical quality of this material have not been available until recently, there is very little data available on the optical properties of BeO. Measurements of the growth of the optical absorption at 2000 Å were made at ambient temperature and at a current density of 1 microamp/cm<sup>2</sup>. The absorption coefficient was observed to increase to 2 cm<sup>-1</sup> and saturate at this value. After an elapsed time of 600 sec at 1 microamp/cm<sup>2</sup>, the absorption coefficients at 1900 Å and 2500 Å were 2 cm<sup>-1</sup> and 1.4 cm<sup>-1</sup>, respectively, while the absorption at 2150 Å and 2300 Å was negligible. In order to make high-dose-rate measurements with a crystal of such small dimensions, it was necessary to operate at a wavelength of 2500 Å where adequate optical signal was available. The temporal variation of the induced absorption coefficient at 2500 Å in BeO during 1.5 Mev electron irradiation at 20 and 30

microamp/cm<sup>2</sup> is shown in Fig. 24. The absorption coefficient rises rapidly after turn-on of the electron beam and then decreases to a steady-state value after the temperature has reached equilibrium. The corresponding steady-state values were 0.5 cm<sup>-1</sup> at 20 microamp/cm<sup>2</sup> and 240 deg C, and 0.8 cm<sup>-1</sup> at 30 microamp/cm<sup>2</sup> and 360 deg C.

These measurements should be taken as preliminary data since only one crystal of very small dimensions was investigated. However, these results are promising, in that the measured levels of absorption were not prohibitive and the specimen did not fracture during irradiation due to thermal shock. It should also be mentioned that the crystal was not visibly colored as a result of this irradiation history.

## DISCUSSION OF RESULTS

The results of measurements of the optical transmission of Amersil and Spectrosil high purity fused silica during 1.5 Mev electron irradiation and following reactor irradiation indicate that these grades of fused silica are similar to Corning 7940 UV grade with regard to the irradiation-induced optical absorption in the wavelength interval from 2000 to 3000 Å. Furthermore, the measured generation, thermal annealing, radiation annealing, and optical bleaching rates of the 2150 Å absorption band in these grades were in essential agreement with those measured in previous programs on Corning 7940 UV grade. Thus, with respect to their optical transmission characteristics, any one of these three high-purity grades of fused silica would be suitable for use as the transparent wall material for the full-scale nuclear light bulb engine.

Measurements of the effects of reactor and 1.5 Mev electron irradiation on the optical transmission of aluminum oxide, although less extensive than the measurements on fused silica, indicate that this material may be acceptable for use as a transparent wall material. It was found during this and the FY 1970 experimental program that 1.5 Mev electron irradiation does not generate appreciable optical absorption in this material. However, reactor irradiation does generate a strong optical absorption band in aluminum oxide that is centered at 2050 Å. This suggests that the color centers associated with this absorption band are caused by the displacement of atoms by fast neutrons rather than ionization of atoms, as in fused silica. This absorption band can be annealed at a temperature of 500 C in the absence of irradiation. Further, measurements made in the present program indicate that this absorption band can be annealed at temperatures below 100 C during 1.5 Mev electron irradiation. This radiation annealing of the 2050 Å absorption band in aluminum oxide is similar to the radiation annealing effects observed in fused silica. As such, coupled with its thermal annealing properties, it may be possible to reduce the level of optical absorption due to neutron damage to an acceptable level in aluminum oxide. In addition, aluminum oxide has a higher melting point and a slightly higher thermal conductivity than fused silica (See Table I). However, its sensitivity to thermal shock, and the difficulty involved in its fabrication may preclude its use in the nuclear light bulb engine.

The results of measurements of the optical transmission of the fluorides (magnesium, barium and lithium) during 1.5 Mev electron irradiation indicate that the level of irradiation-induced optical absorption in these materials is excessive at radiation levels considerably lower than those expected in the full-scale nuclear light bulb engine. The resulting heat load on the transparent wall due to this irradiation-induced optical absorption and the questionable structural integrity of each of these materials indicates that they would not be suitable transparent wall materials.

A single crystal specimen of beryllium oxide was investigated during the present program. This material is of considerable interest as a transparent wall material due to its excellent optical transmission and thermal properties (see Table I). In single crystal form this material has an ultraviolet transmission cutoff near 1200 Å, and an extremely high melting point of 2800 C. In addition, the thermal conductivity of beryllium oxide is approximately 2 watts/cm-deg; extremely high for a dielectric material and about two orders of magnitude higher than that of fused silica. Data on the optical properties of beryllium oxide, and in particular the effects of nuclear radiation on the optical transmission, is very limited at present. This is due primarily to the lack of single crystals of good optical quality. The measurements made during the present program are most encouraging in that the results indicated a low level of irradiation-induced optical absorption. In particular, the steady-state irradiation-induced absorption coefficient at 2500 Å was  $0.8 \text{ cm}^{-1}$  at an ionizing dose rate of 3.5 Mrad/sec and a temperature of 360 C. Thus, further measurements of the optical transmission of single crystal beryllium oxide, involving a larger number of specimens, are recommended since it exhibits considerable promise as a transparent wall material for the nuclear light bulb engine.

## REFERENCES

1. Compton, W. D. and G. W. Arnold, Jr.: Radiation Effects in Fused Silica and  $\alpha$ - $\text{Al}_2\text{O}_3$ . Disc Faraday Soc. 31, 130 (1961).
2. Nelson, C. M. and J. H. Crawford, Jr.: Optical Absorption in Irradiated Quartz and Fused Silica. J. Phys. Chem. Sol. 13, 296 (1960).
3. Nelson, C. M. and R. A. Weeks: Trapped Electrons in Irradiated Quartz and Silica. Journal of the American Ceramic Society 43, 396 (1960).
4. Nelson, C. M. and R. A. Weeks: Vacuum-Ultraviolet Absorption Studies of Irradiated Silica and Quartz. Journal of Applied Physics 32, 883 (1961).
5. Levy, P. W.: Reactor and Gamma-Ray Induced Coloring of Corning Fused Silica. J. Phys. Chem. Sol. 13, 287 (1960).
6. Gagosz, R. M., F. C. Douglas and M. A. DeCrescente: Optical Absorption in Transparent Materials Following High-Temperature Reactor Irradiation. United Aircraft Research Laboratories Report F-910485-2, September 1967. Also issued as NASA CR-1032.
7. Gagosz, R. M., J. P. Waters, F. C. Douglas and M. A. DeCrescente: Optical Absorption in Fused Silica during Triga Reactor Pulse Irradiations. United Aircraft Research Laboratories Report F-910485-1, September 1967. Also issued as NASA CR-1031.
8. Gagosz, R. M. and J. P. Waters: Optical Absorption and Fluorescence in Fused Silica during Triga Pulse Irradiations. United Aircraft Research Laboratories Report G-910485-3, April 1968. Also issued as NASA CR-1191.
9. Palma, G. E. and R. M. Gagosz: Optical Absorption in Fused Silica during Irradiation at High Temperature. United Aircraft Research Laboratories Report H-930709-1, October 1969.
10. Palma, G. E. and R. M. Gagosz: Optical Absorption in Transparent Materials during 1.5 Mev Electron Irradiation. United Aircraft Research Laboratories Report J-990929-1, October 1970.
11. Sullivan, J. O. and A. C. Holland: A Congeries of Absorption Cross Section for Wavelengths Less than 3000 Å. NASA CR-371, January 1966.
12. Corbett, J. W.: Electron Radiation Damage in Semiconductors and Metals, pp. 30-36, Academic Press, New York and London (1966).



K990929-2

13. Heath, D. F. and P. A. Sacher: Effects of a Simulated High-Energy Space Environment on the Ultraviolet Transmittance of Optical Materials between 1050 Å and 3000 Å. Applied Optics 5, 937 (1966).

## LIST OF SYMBOLS

|                             |   |
|-----------------------------|---|
| A                           | Atomic weight, dimensionless  |
| D                           | Ionizing dose, Mrad   |
| $\dot{D}$                   | Ionizing dose rate, Mrad/sec  |
| E                           | Electron kinetic energy, Mev  |
| $I_0(\lambda)$              | Chart recorder amplitude prior to irradiation, dimensionless                |
| $I(\lambda, T, \dot{D}, t)$ | Chart recorder amplitude during irradiation, dimensionless                  |
| J                           | Current density, microamp/cm <sup>2</sup>                                   |
| $\ell$                      | Optical path length, cm   |
| t                           | Elapsed time, sec   |
| T                           | Specimen temperature, deg C   |
| Z                           | Atomic number, dimensionless  |
| $\alpha(\lambda)$           | Induced absorption coefficient at a wavelength $\lambda$ , cm <sup>-1</sup> |
| $\alpha(\lambda)/\alpha_p$  | Normalized absorption coefficient, dimensionless                            |
| $\lambda$                   | wavelength, Å   |
| $\lambda_{IR}$              | Infrared cutoff wavelength, Å   |
| $\lambda_{UV}$              | Ultraviolet cutoff wavelength, Å  |
| $\rho$                      | Density, gm/cm <sup>3</sup>   |
| $T_A(T)$                    | Thermal annealing time constant, sec  |

TABLE I

## IMPORTANT PROPERTIES OF CANDIDATE TRANSPARENT WALL MATERIALS

| <u>Material</u>                | <u>Transmission Window</u><br><u><math>\lambda_{IR} - \lambda_{UV}</math> (Microns)</u> | <u>Melting Point</u><br><u>Deg C</u> | <u>Thermal</u><br><u>Conductivity</u><br><u>Watts/cm-C<sup>o</sup></u> |
|--------------------------------|---|--------------------------------------|--|
| SiO <sub>2</sub>               | 4 - 0.16  | 1450                                 | 0.016  |
| Al <sub>2</sub> O <sub>3</sub> | 6 - 0.14  | 2050                                 | 0.026  |
| BaF <sub>2</sub>               | 12 - 0.13   | 1320                                 | 0.11   |
| MgF <sub>2</sub>               | 7.5 - 0.12  | 1310                                 | 0.12   |
| LiF                            | 6.2 - 0.11  | 870                                  | 0.11   |
| BeO                            | 4 - 0.12 <sup>†</sup>   | 2800                                 | 2.0  |

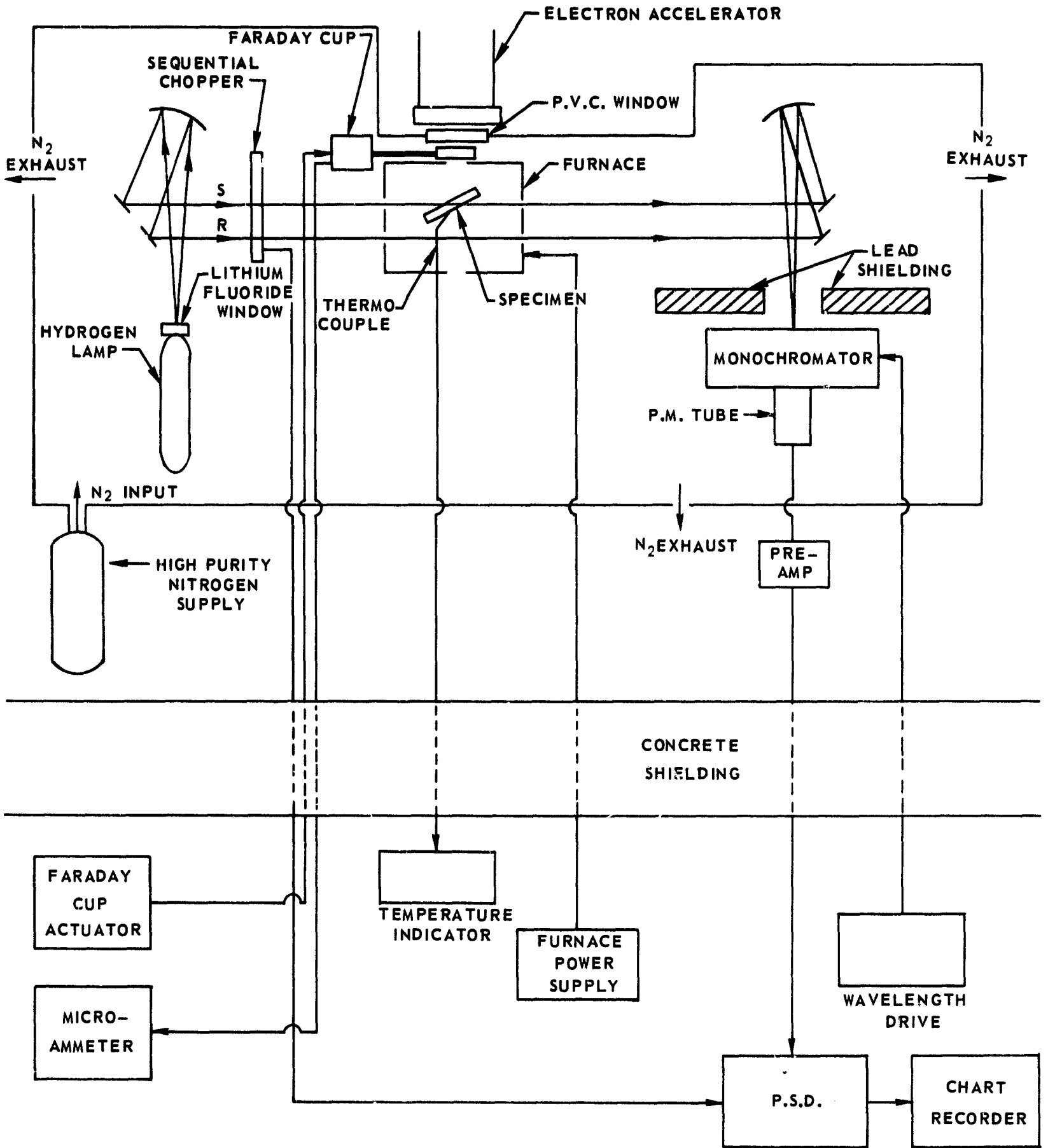
† Private Communication with S. B. Austerman of North American Autonetics Corp.

TABLE II

RELATION BETWEEN IONIZING DOSE RATE AND CURRENT DENSITY  
FOR SEVERAL MATERIALS AT AN ELECTRON ENERGY OF 1.5 Mev.

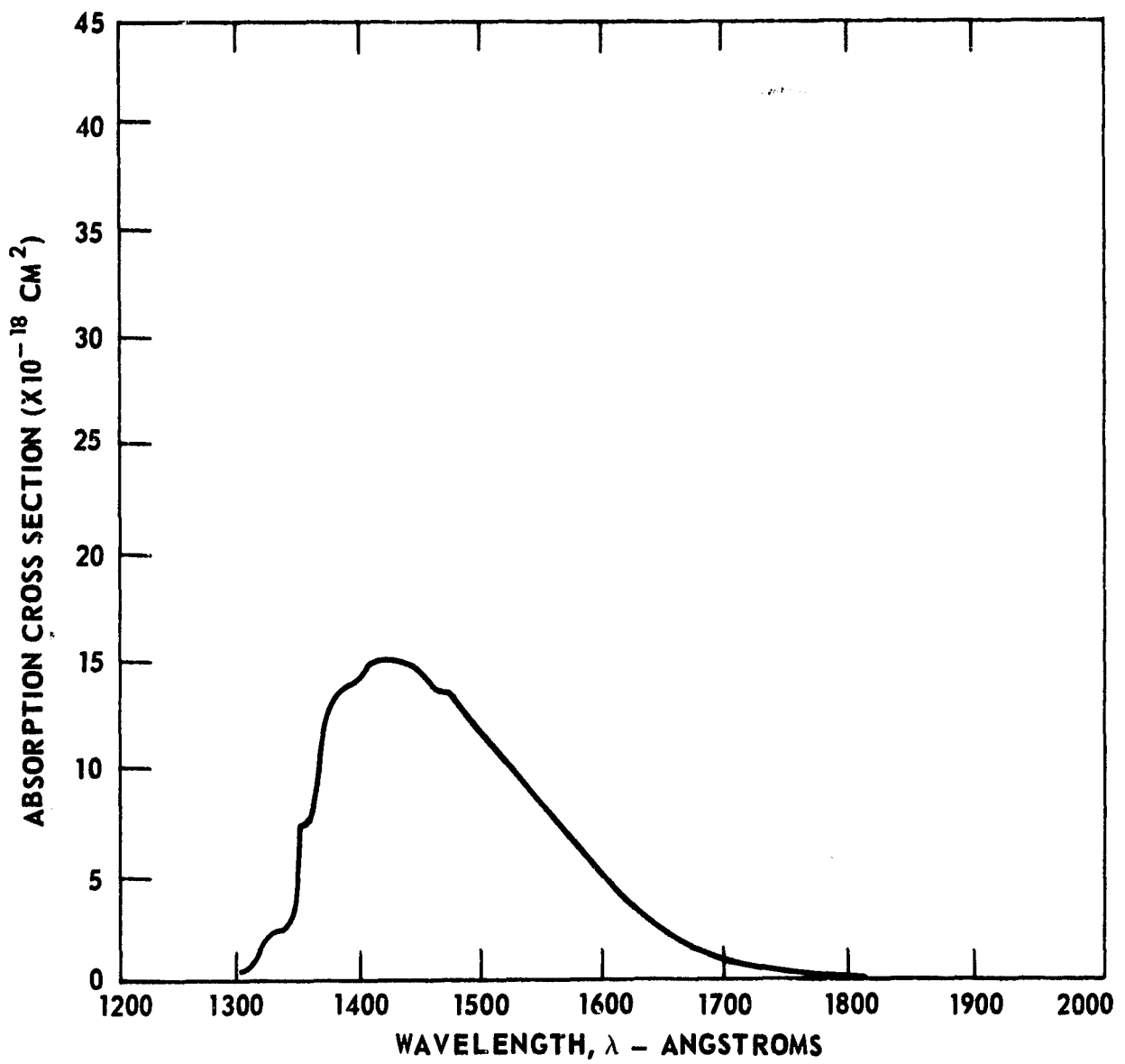
| <u>Material</u>                | <u>Density<br/>(Gm/cm<sup>3</sup>)</u> | <u>Average Atomic<br/>Number Z</u> | <u>Average Atomic<br/>Weight A</u> | <u><math>\dot{D}/J</math><br/>(Mrad/microamp-sec)</u> |
|--------------------------------|--|------------------------------------|------------------------------------|---|
| SiO <sub>2</sub>               | 2.2                                    | 10                                 | 20                                 | 0.125   |
| Al <sub>2</sub> O <sub>3</sub> | 4.0                                    | 10                                 | 20.4                               | 0.14  |
| BaF <sub>2</sub>               | 4.82                                   | 24.7                               | 58                                 | 0.13  |
| MgF <sub>2</sub>               | 3.18                                   | 10                                 | 20.7                               | 0.11  |
| LiF                            | 2.64                                   | 6                                  | 13                                 | 0.12  |
| BeO                            | 3.0                                    | 6                                  | 12.5                               | 0.11  |

### ELECTRICAL AND OPTICAL SCHEMATIC FOR ELECTRON IRRADIATION EXPERIMENTS



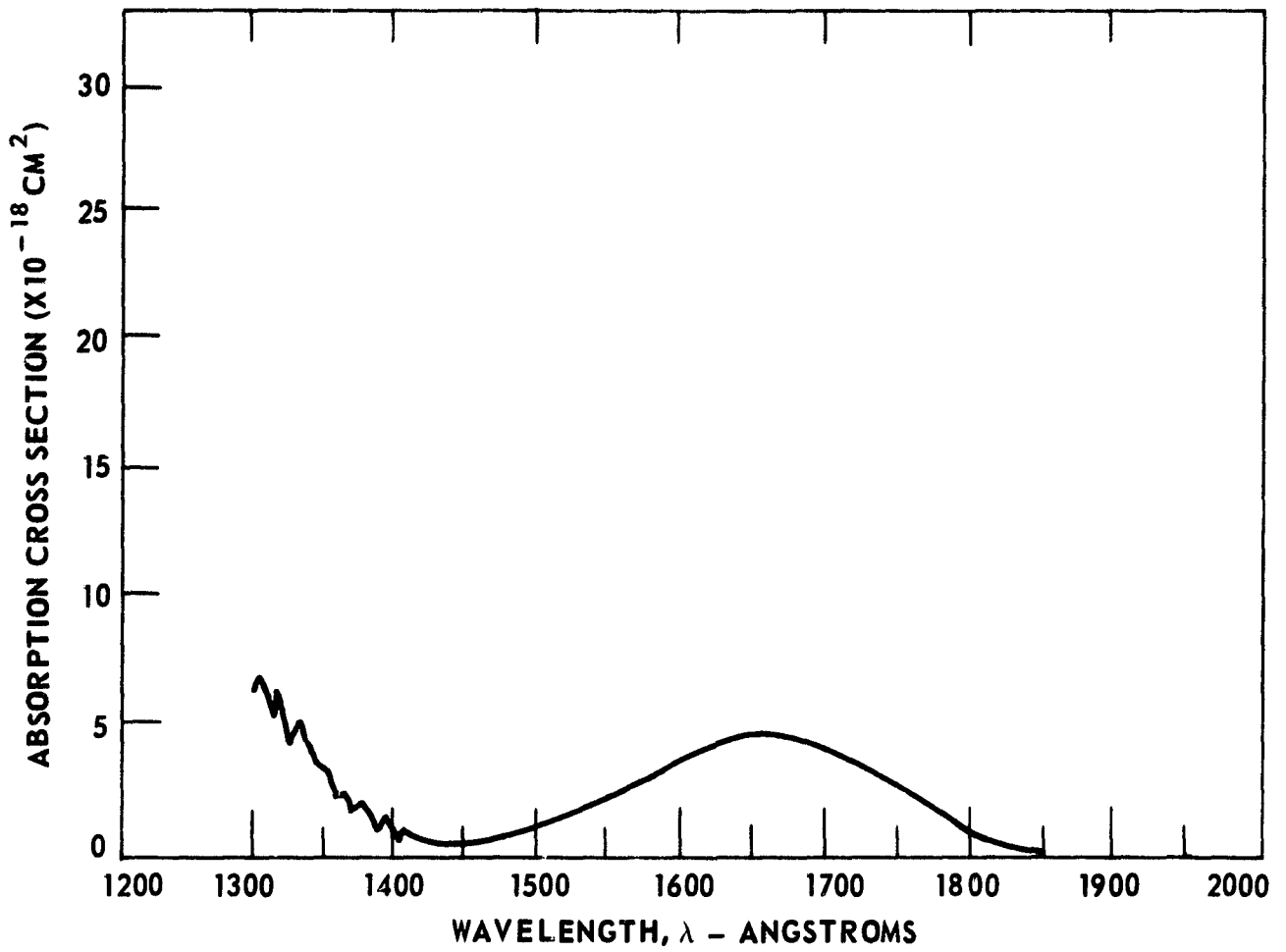
ABSORPTION CROSS SECTION OF O<sub>2</sub>

1300-1800 Å



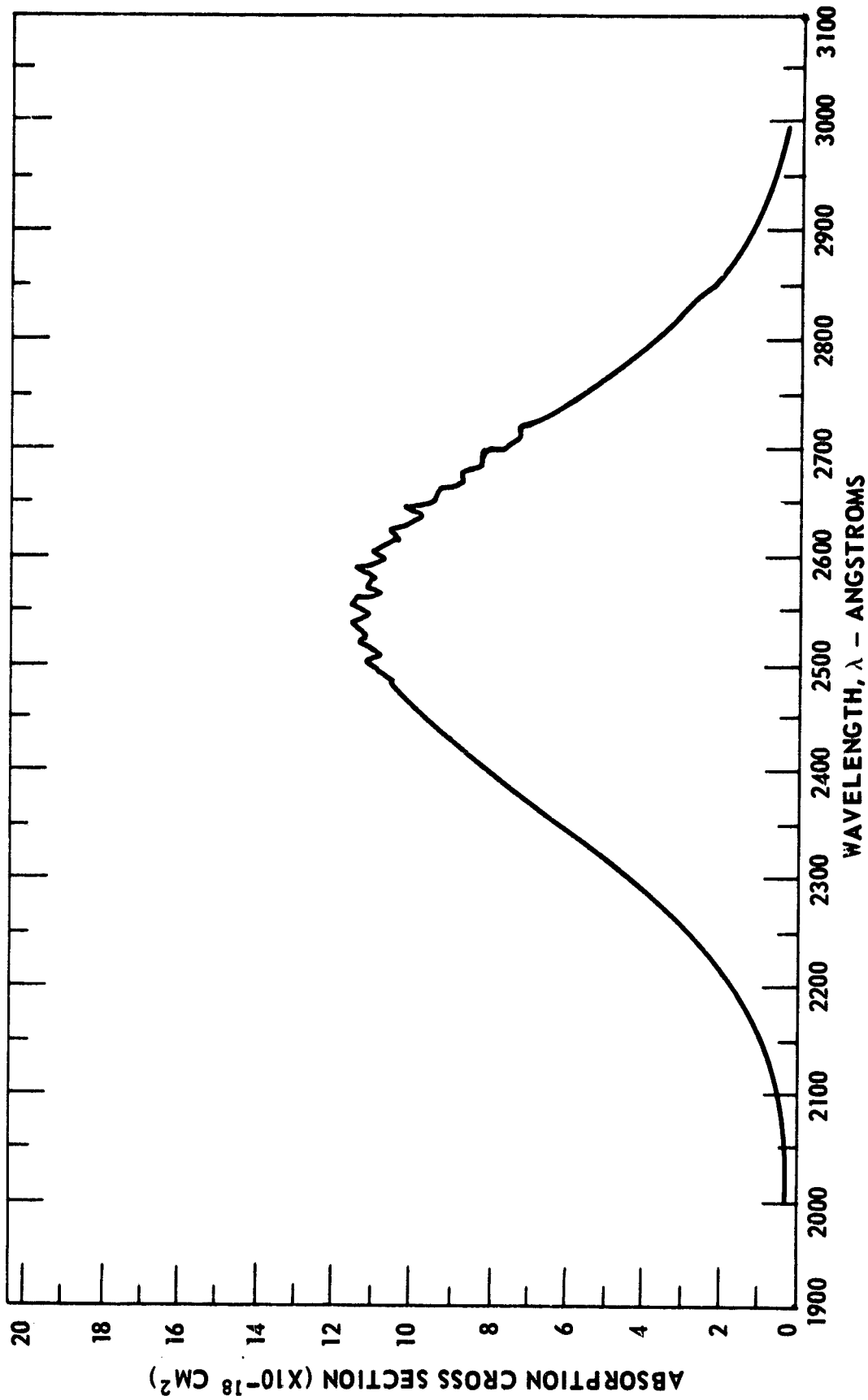
### ABSORPTION CROSS SECTION OF H<sub>2</sub>O

1300-1850 Å



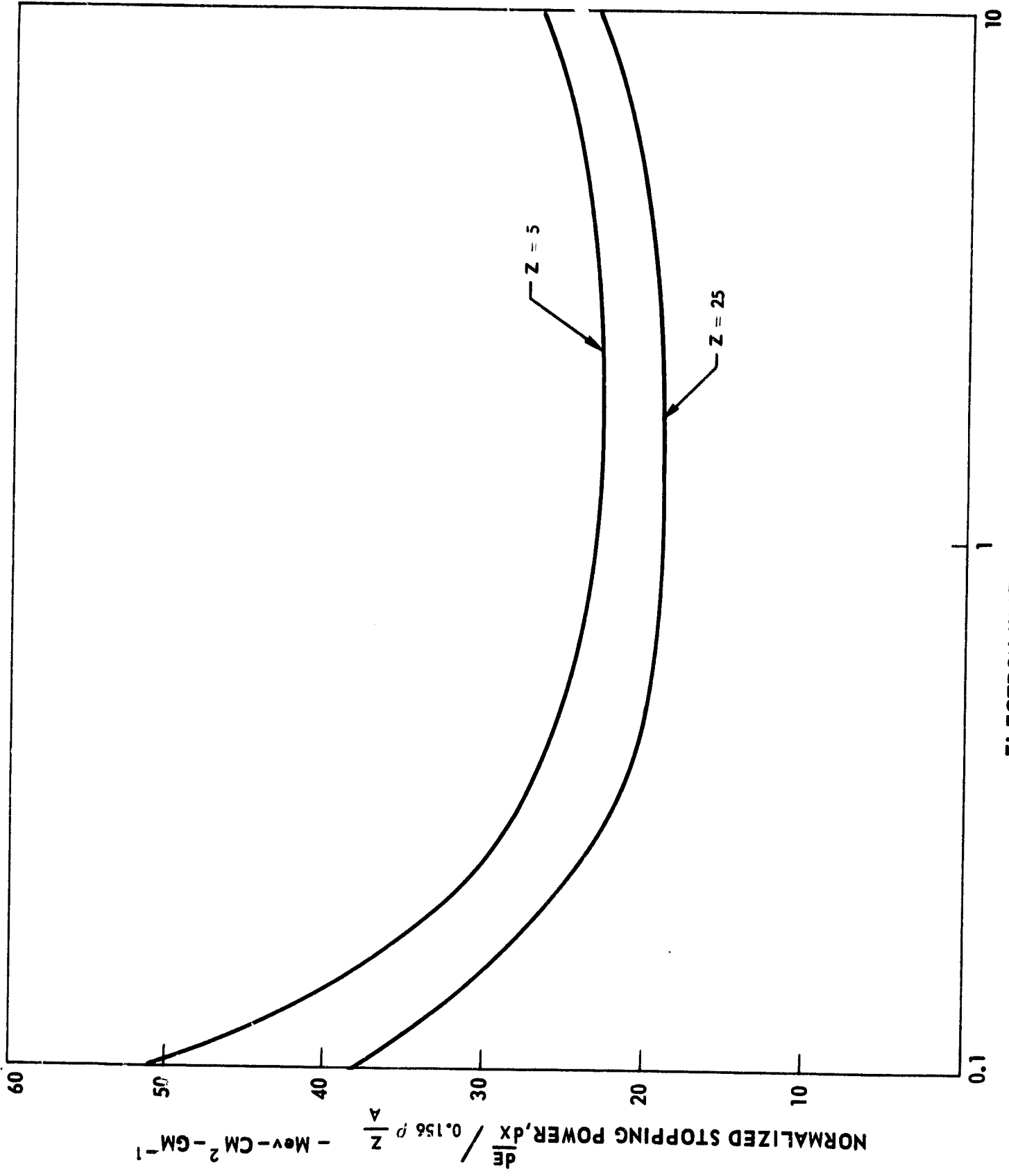
# ABSORPTION CROSS SECTION OF O<sub>3</sub>

2000-3000 Å





VARIATION OF STOPPING POWER WITH ELECTRON KINETIC ENERGY



ELECTRON KINETIC ENERGY, E - Mev

# GROWTH OF INDUCED ABSORPTION FOR AMERSIL SPECIMEN A-1 DURING 1.5 Mev ELECTRON IRRADIATION

$\lambda = 2150 \text{ \AA}$

$\dot{D} = 0.05 \text{ MRAD/SEC}$

$T = 40 \text{ C}$

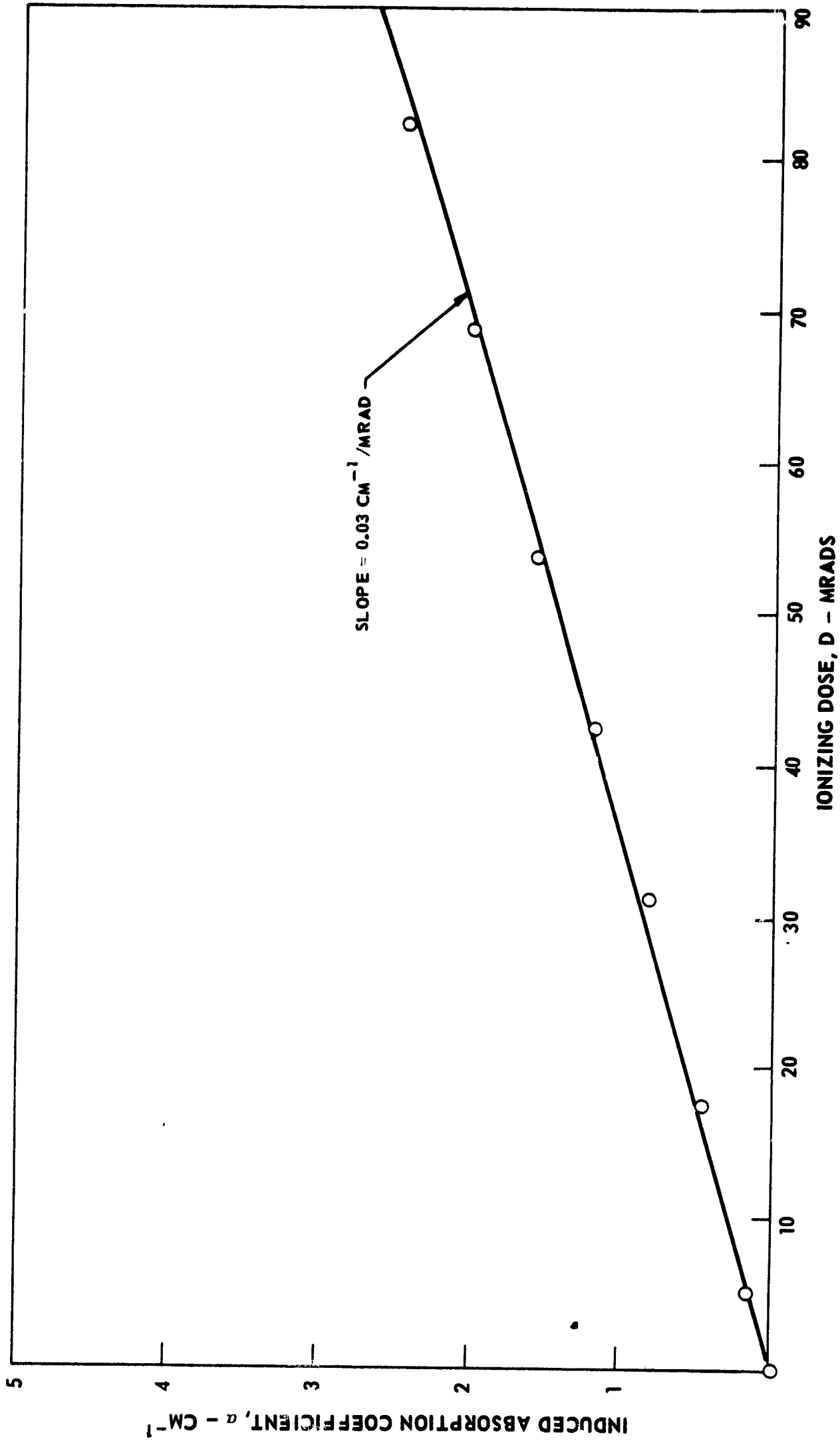


FIG. 6

# GROWTH OF INDUCED ABSORPTION FOR SPECTROSIL SPECIMEN S-1 DURING 1.5 Mev ELECTRON IRRADIATION

$\lambda = 2150 \text{ \AA}$

$\dot{D} = 0.05 \text{ MRAD/SEC}$

$T = 40 \text{ C}$

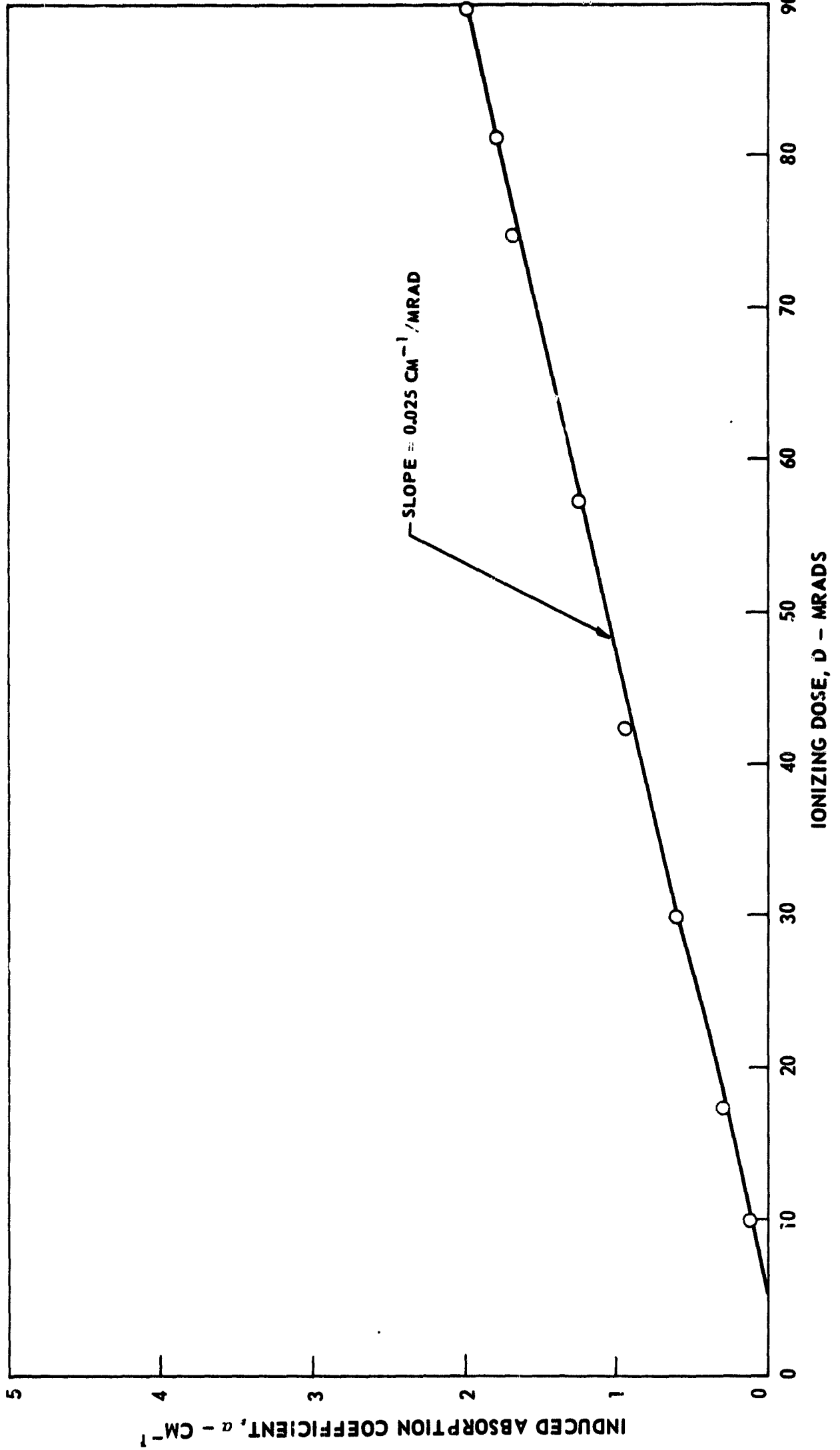


FIG. 7

RADIATION ANNEALING OF REACTOR-IRRADIATION-INDUCED ABSORPTION AT  
2150 Å OF AMERSIL SPECIMEN AN-1

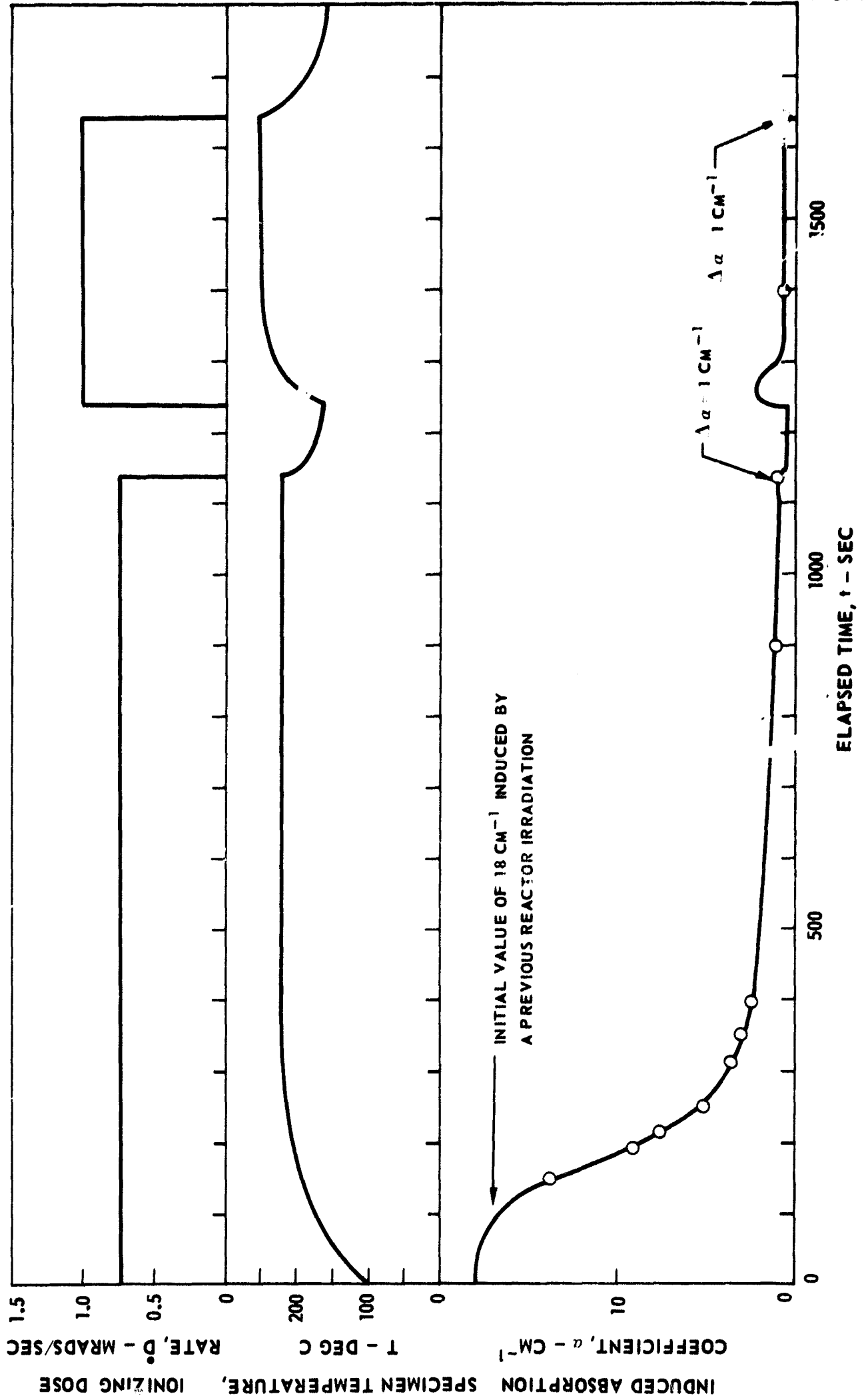
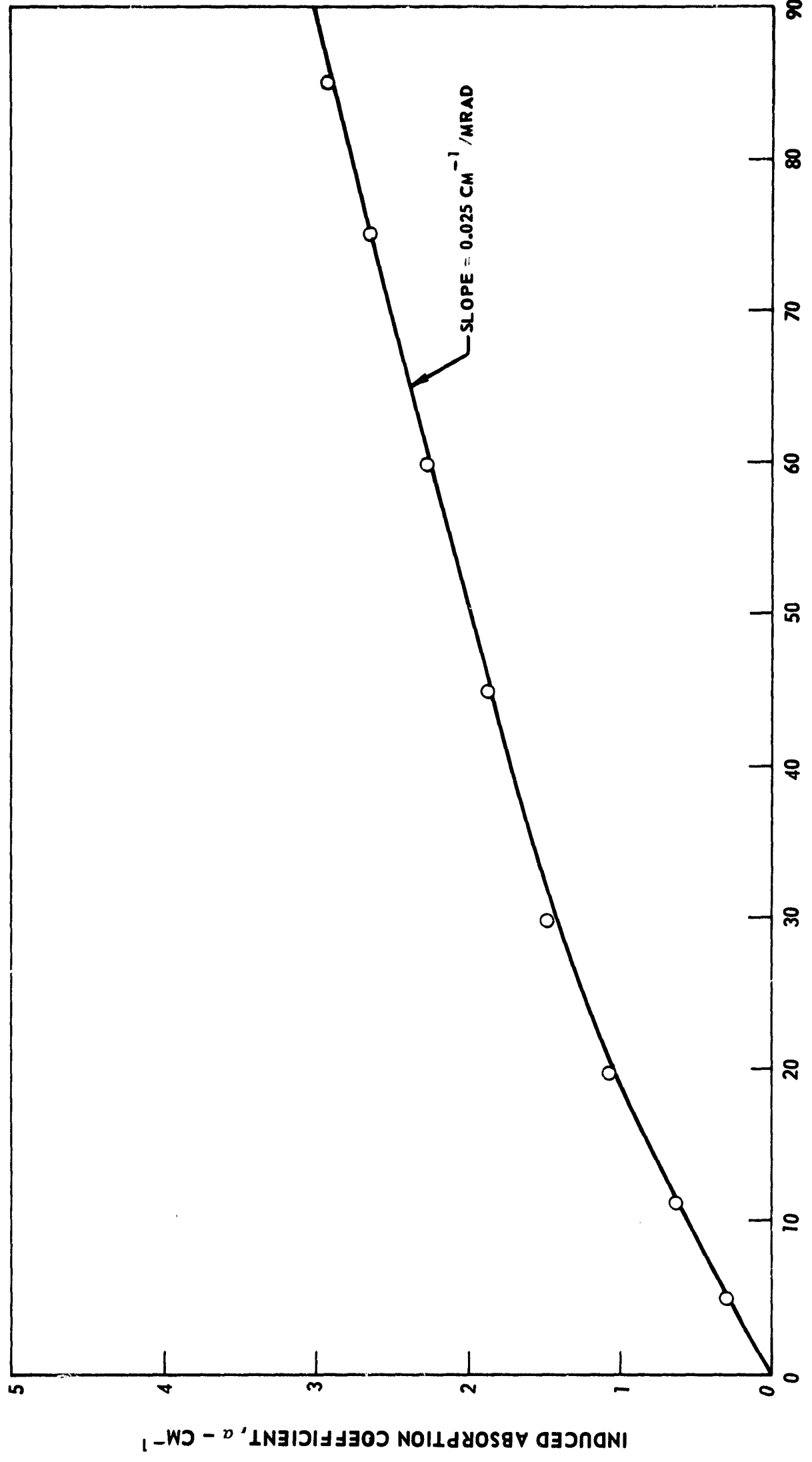


FIG. 8

# GROWTH OF INDUCED ABSORPTION FOR AMERSIL SPECIMEN AN-1 DURING 1.5 Mev ELECTRON IRRADIATION AFTER RADIATION ANNEALING

$\lambda = 2150 \text{ \AA}$   
 $\dot{D} = 0.05 \text{ MRAD/SEC}$   
 $T = 40 \text{ C}$



# RADIATION ANNEALING OF REACTOR-IRRADIATION-INDUCED ABSORPTION AT 2150 Å OF SPECTROSIL SPECIMEN SN-1

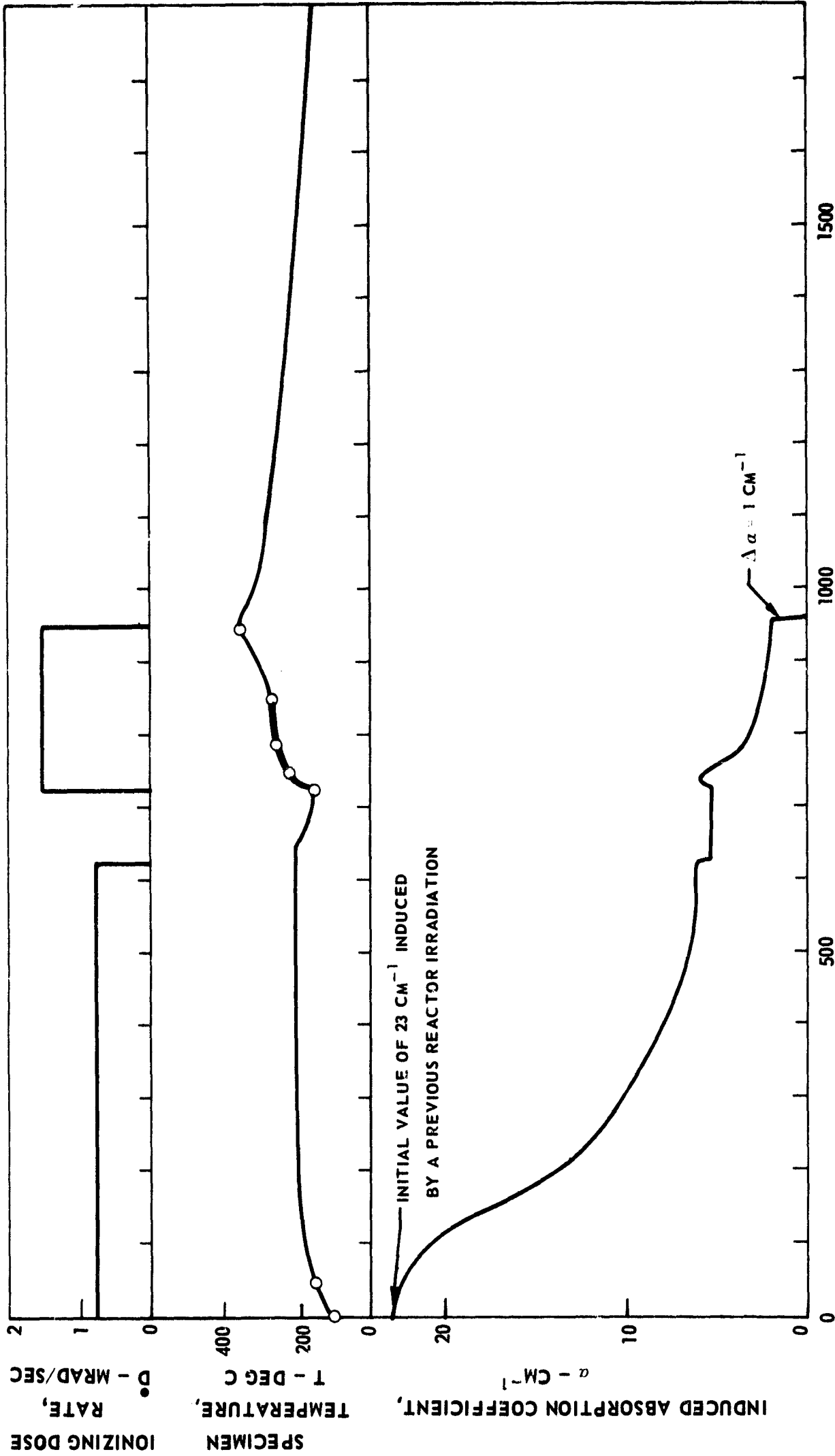


FIG. 10

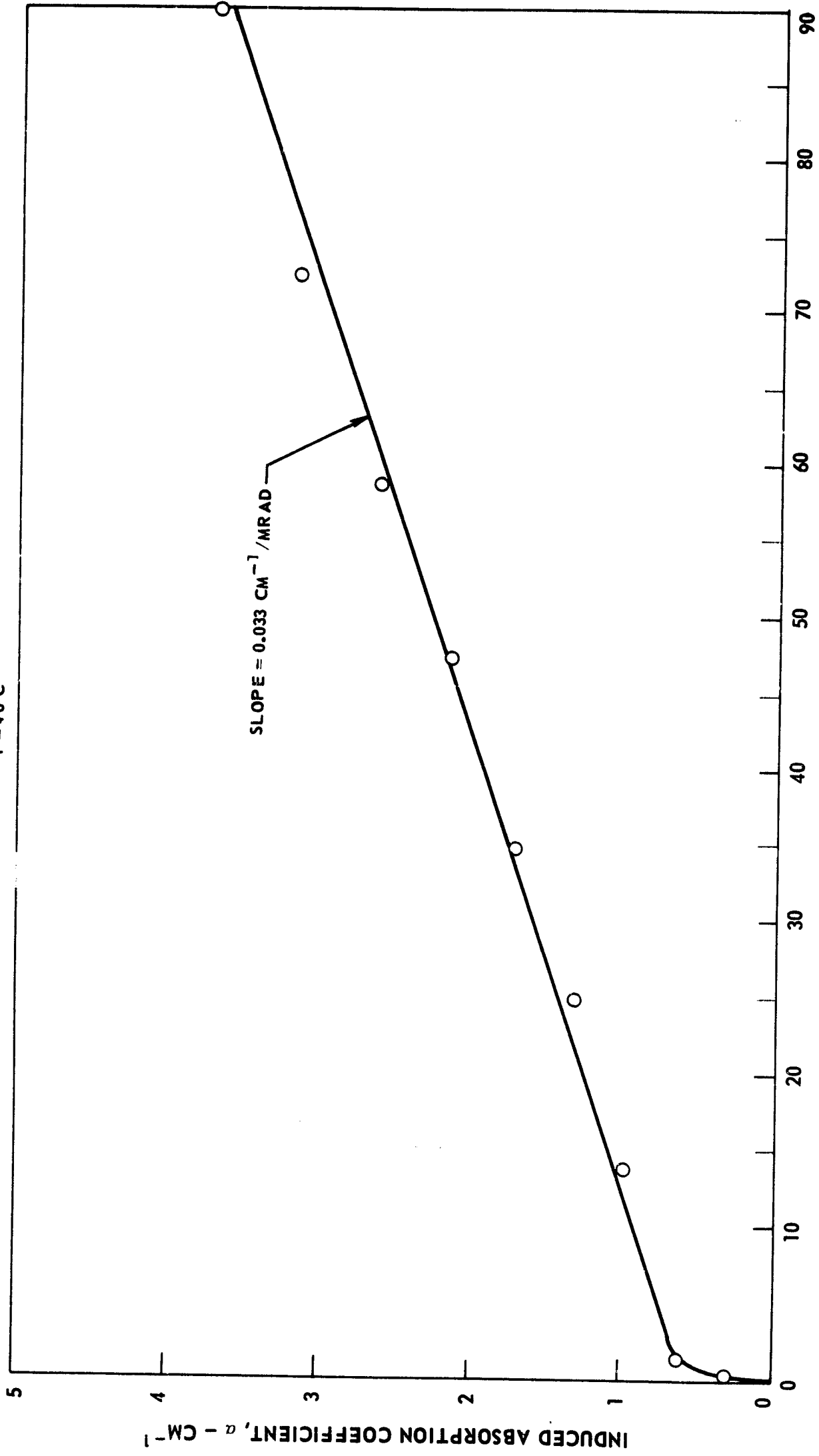
ELAPSED TIME, t - SEC

# GROWTH OF INDUCED ABSORPTION FOR SPECTROSIL SPECIMEN SN-1 DURING 1.5 Mev ELECTRON IRRADIATION AFTER RADIATION ANNEALING

$\lambda = 2150 \text{ \AA}$

$\dot{D} = 0.05 \text{ MRAD/SEC}$

$T = 40 \text{ C}$



IONIZING DOSE, D - MRADS

FIG. 11

THERMAL ANNEALING OF REACTOR-IRRADIATION-INDUCED ABSORPTION IN FUSED SILICA  
 AMERSIL SPECIMEN AN-2 AT 2150 Å

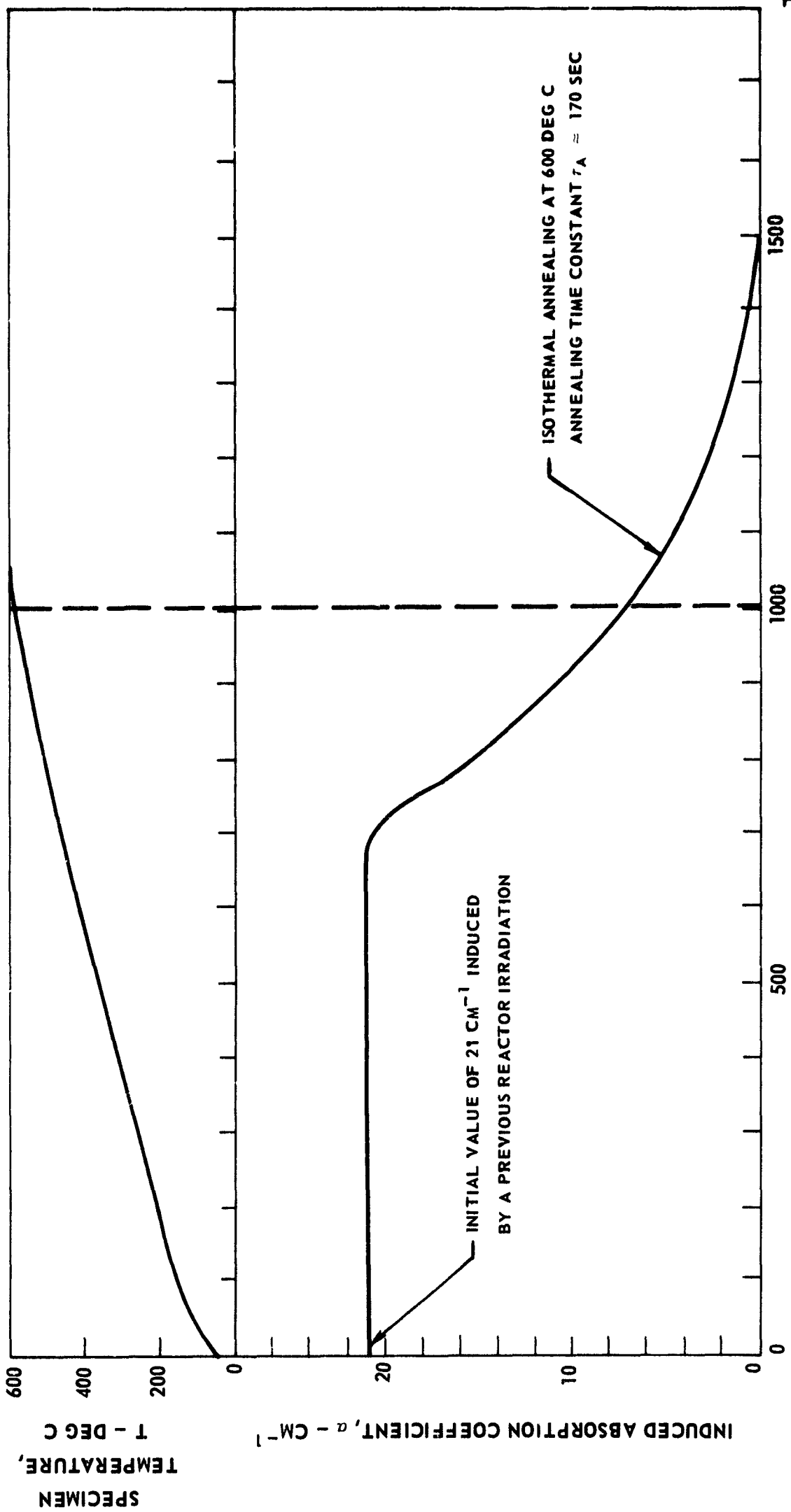


FIG. 12



# GROWTH OF INDUCED ABSORPTION FOR AMERSIL SPECIMEN AN-2 DURING 1.5 Mev ELECTRON IRRADIATION AFTER THERMAL ANNEALING AT 600 C

$\lambda = 2150 \text{ \AA}$   
 $D = 0.05 \text{ MRAD/SEC}$   
 $T = 40 \text{ C}$

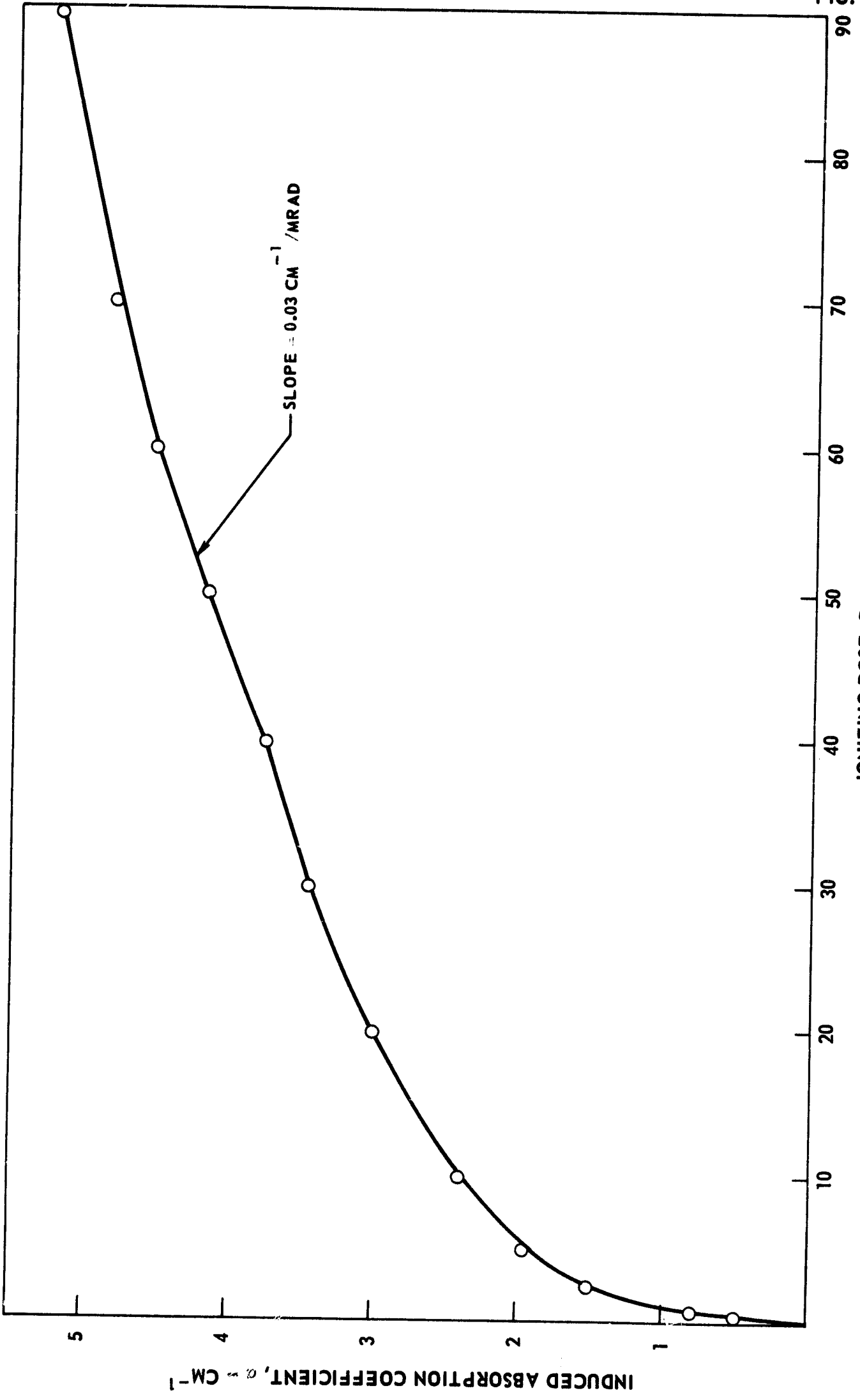


FIG. 13

IONIZING DOSE, D - MRAD

GROWTH OF INDUCED ABSORPTION FOR SPECTROSIL SPECIMEN SN-2 DURING 1.5 Mev ELECTRON IRRADIATION AFTER OPTICAL BLEACHING

$\lambda = 2150 \text{ \AA}$   
 $\dot{D} = 0.05 \text{ MRAD/SEC}$   
 $T = 40 \text{ C}$

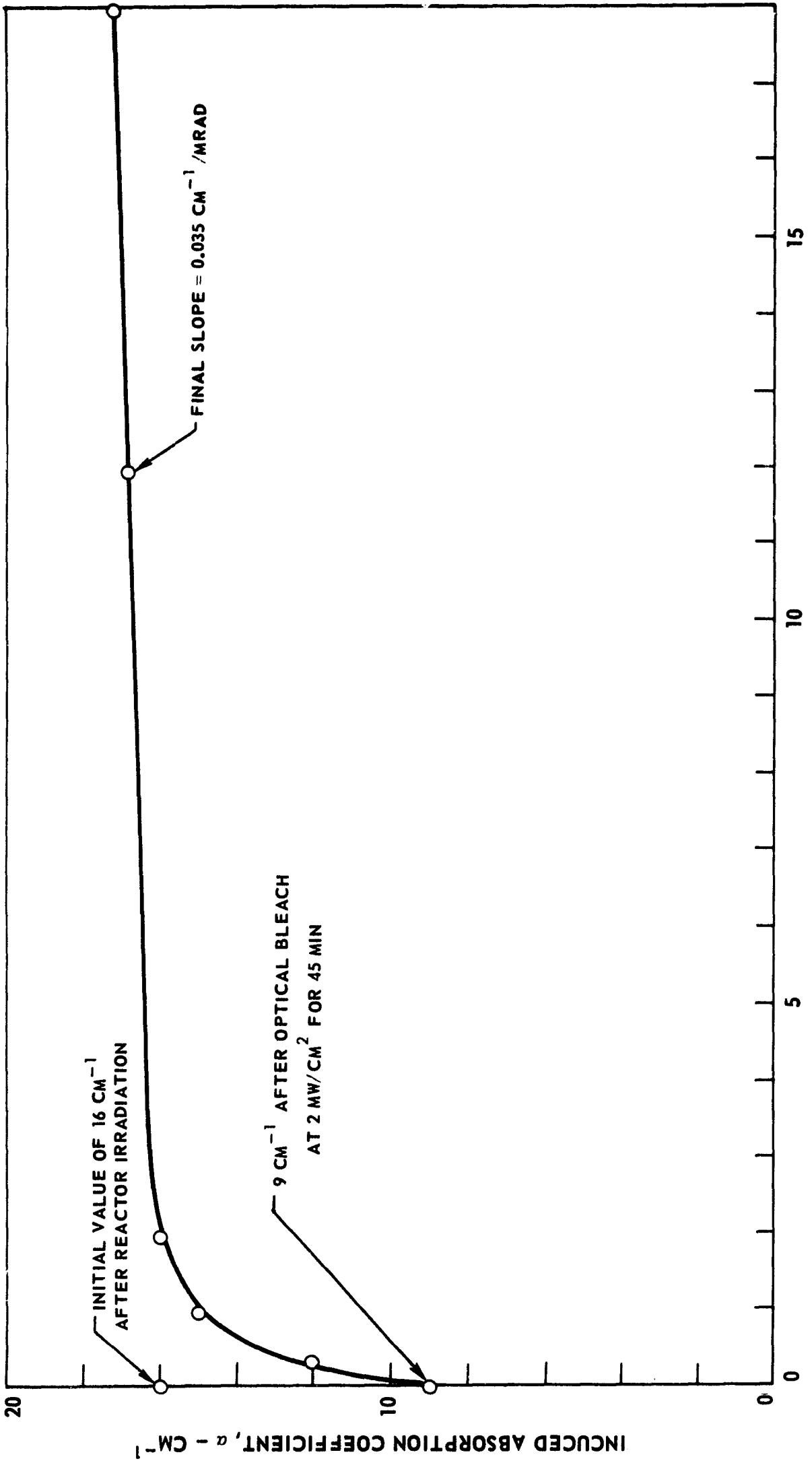
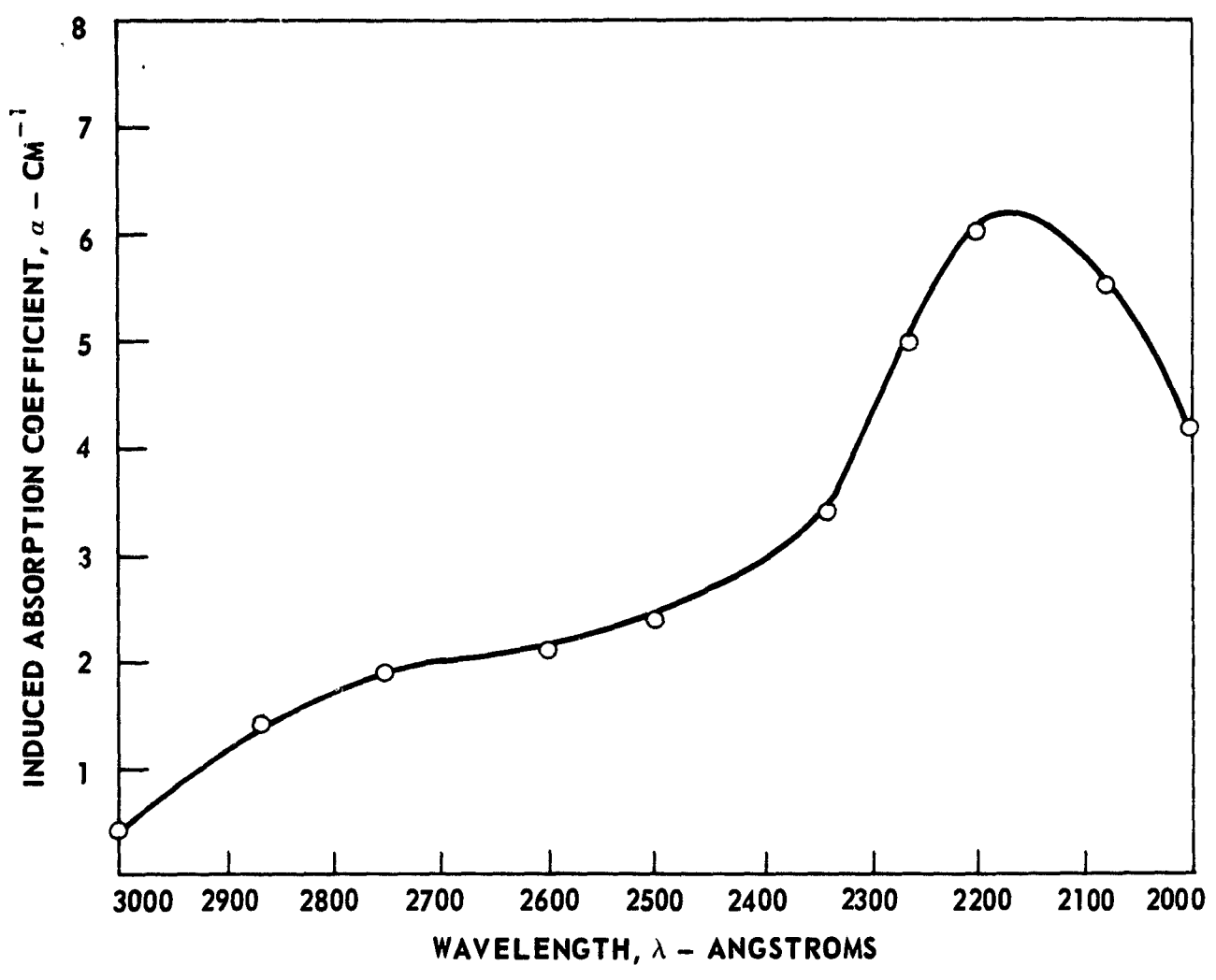


FIG. 14

IONIZING DOSE, D - MRADS

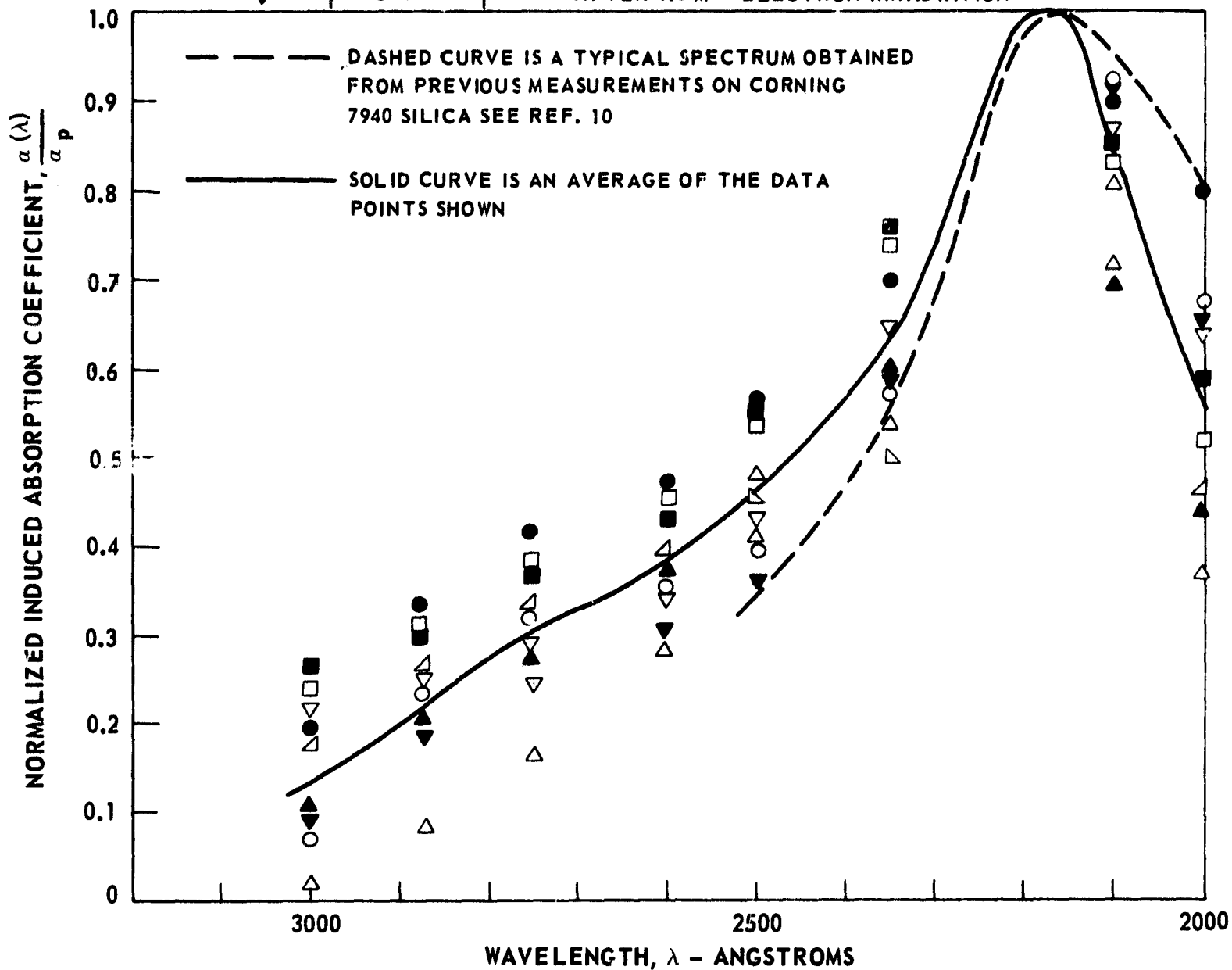
ABSORPTION SPECTRA OF CORNING 7940 FUSED SILICA AFTER 7 Mev ELECTRON IRRADIATION TO A DOSE OF 190 MRAD

$\dot{D} = 0.1 \text{ MRAD/SEC}$   
 $T = 40 \text{ C}$



**NORMALIZED IRRADIATION - INDUCED ABSORPTION SPECTRA OF FUSED SILICA**

| SYMBOL | SPECIMEN | MEASUREMENT CONDITIONS   |
|--------|----------|--|
| ○      | C-1      | AFTER 7 Mev ELECTRON IRRADIATION                                   |
| △      | AN-1     | AFTER REACTOR IRRADIATION  |
| □      | AN-1     | AFTER RADIATION ANNEALING AND REIRRADIATION WITH 1.5 Mev ELECTRONS |
| ▲      | SN-1     | AFTER REACTOR IRRADIATION  |
| ■      | SN-1     | AFTER RADIATION ANNEALING AND REIRRADIATION WITH 1.5 Mev ELECTRONS |
| ◁      | AN-2     | AFTER REACTOR IRRADIATION  |
| ▷      | AN-2     | AFTER THERMAL ANNEALING AND REIRRADIATION WITH 1.5 Mev ELECTRONS   |
| ●      | A-1      | AFTER 1.5 Mev ELECTRON IRRADIATION                                 |
| ▼      | S-1      | AFTER 1.5 Mev ELECTRON IRRADIATION                                 |



# RADIATION ANNEALING OF REACTOR-IRRADIATION-INDUCED ABSORPTION IN ALUMINUM OXIDE

$\lambda = 2950 \text{ \AA}$

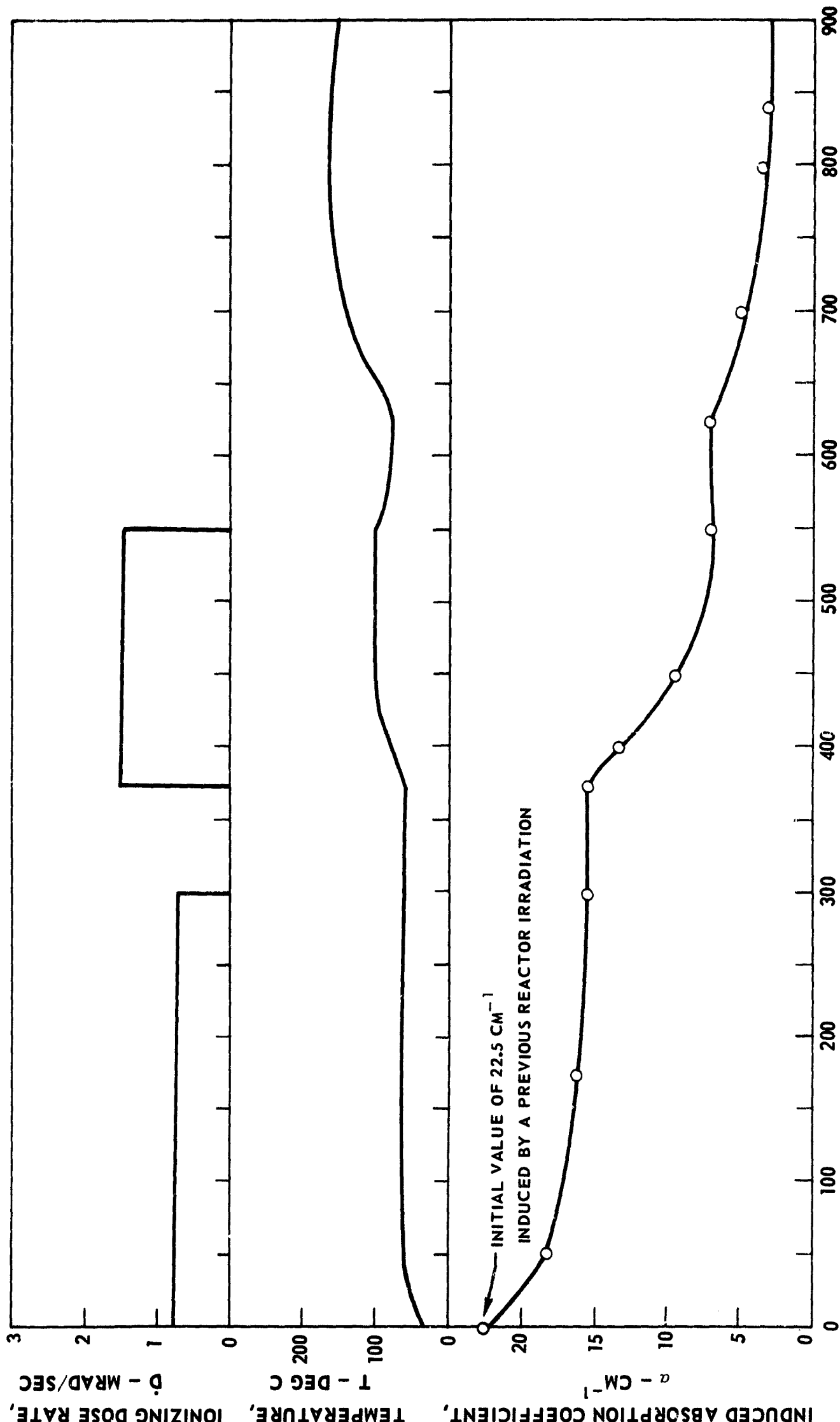
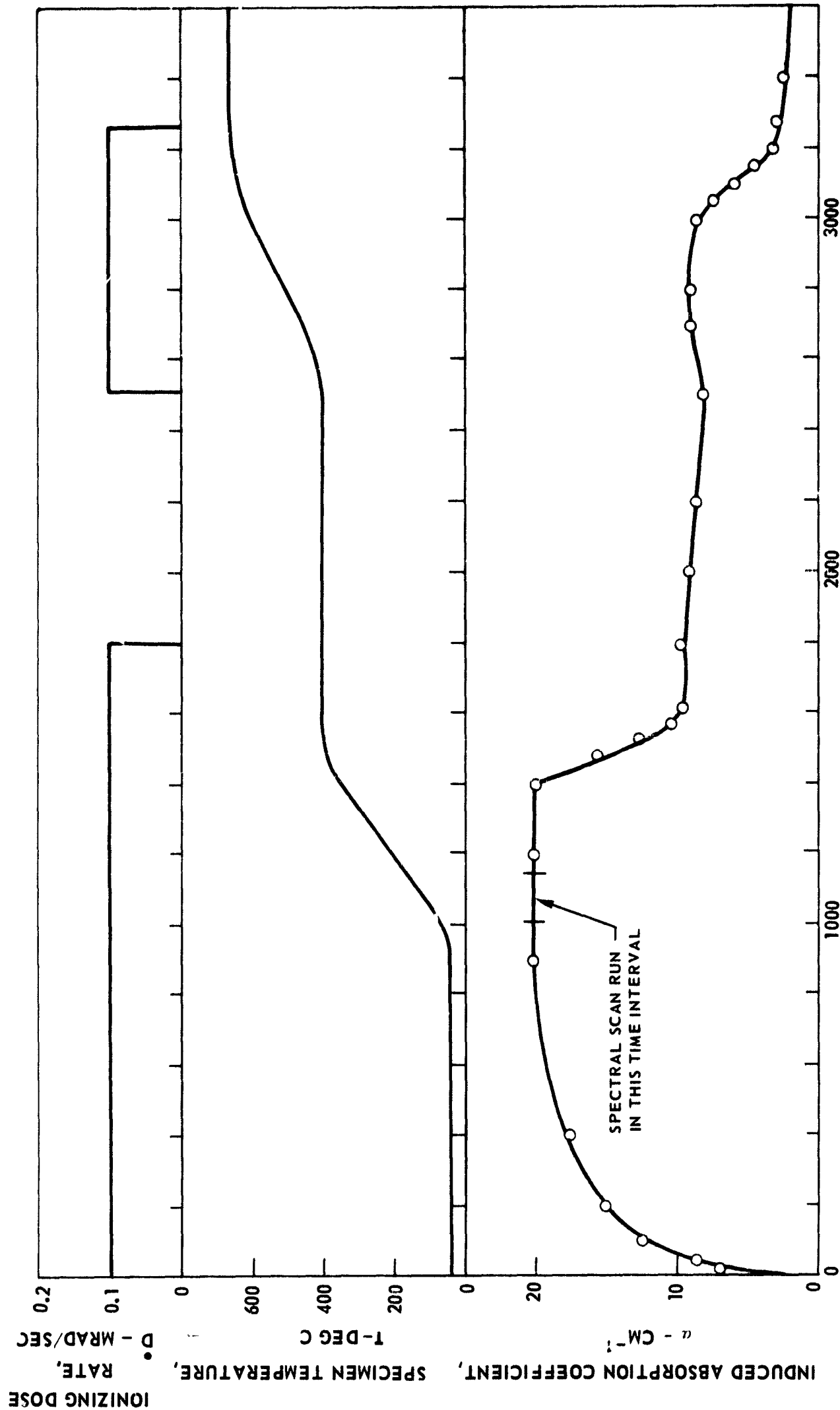


FIG.

IRRADIATION HISTORY OF Mg F<sub>2</sub> SPECIMEN

$\lambda = 2600 \text{ \AA}$

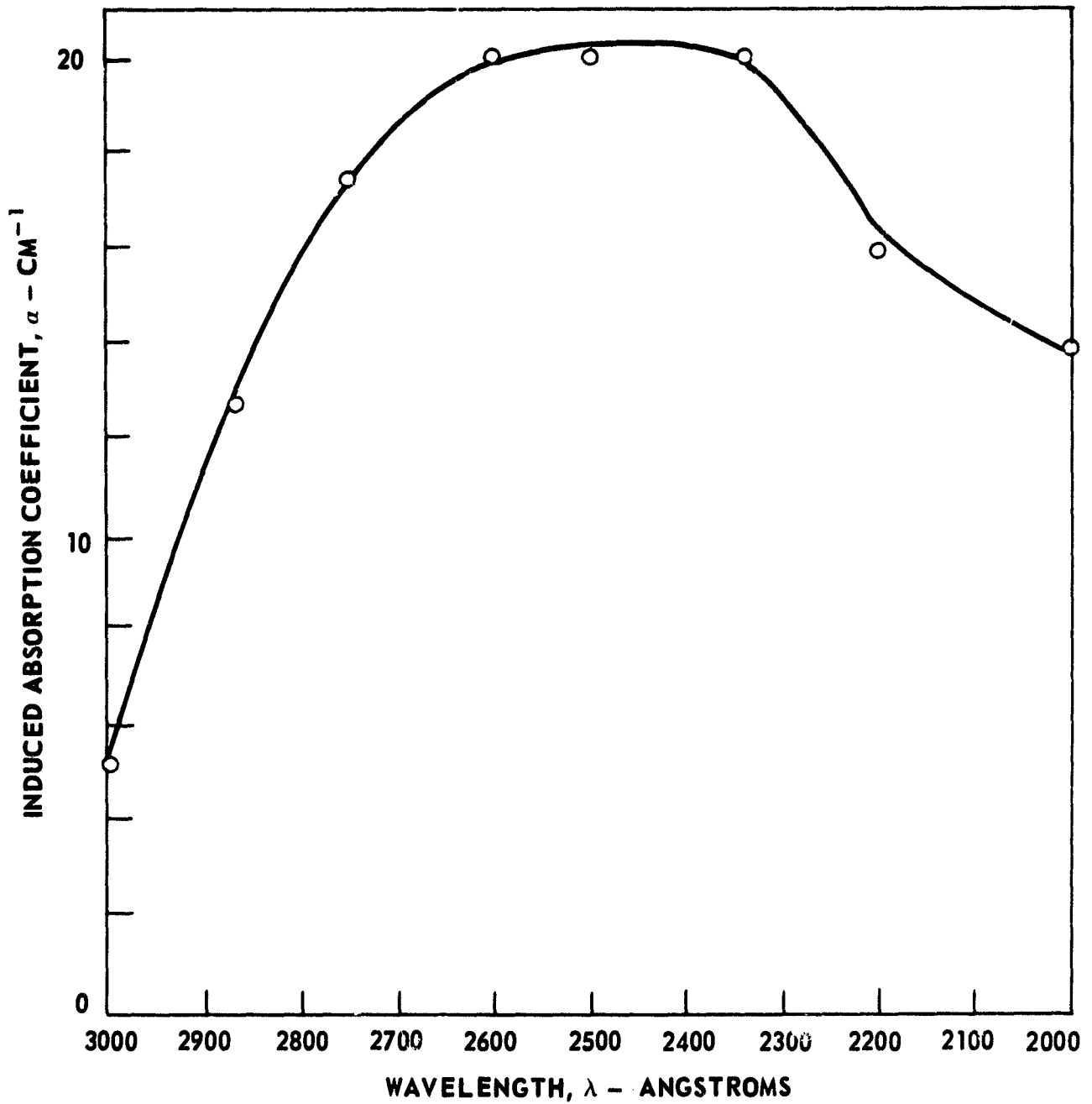


ELAPSED TIME, t - SEC

ABSORPTION SPECTRA OF MAGNESIUM FLUORIDE DURING 1.5 Mev  
ELECTRON IRRADIATION

$\dot{D} = 0.1 \text{ MRAD/SEC}$

$T = 40 \text{ DEG C}$



# IRRADIATION HISTORY OF Ba F<sub>2</sub> SPECIMEN $\lambda$ 2600 Å

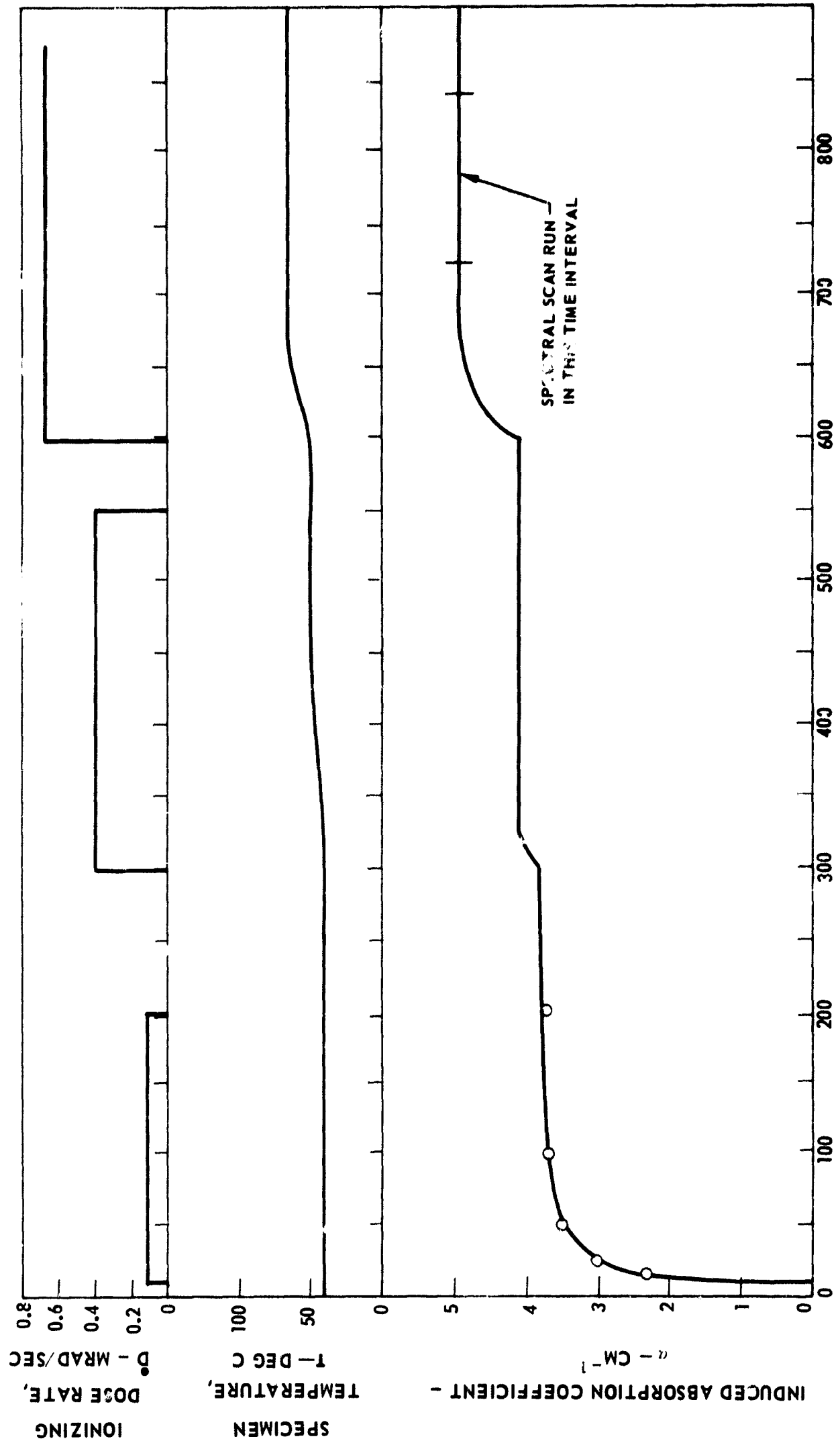


FIG. 20

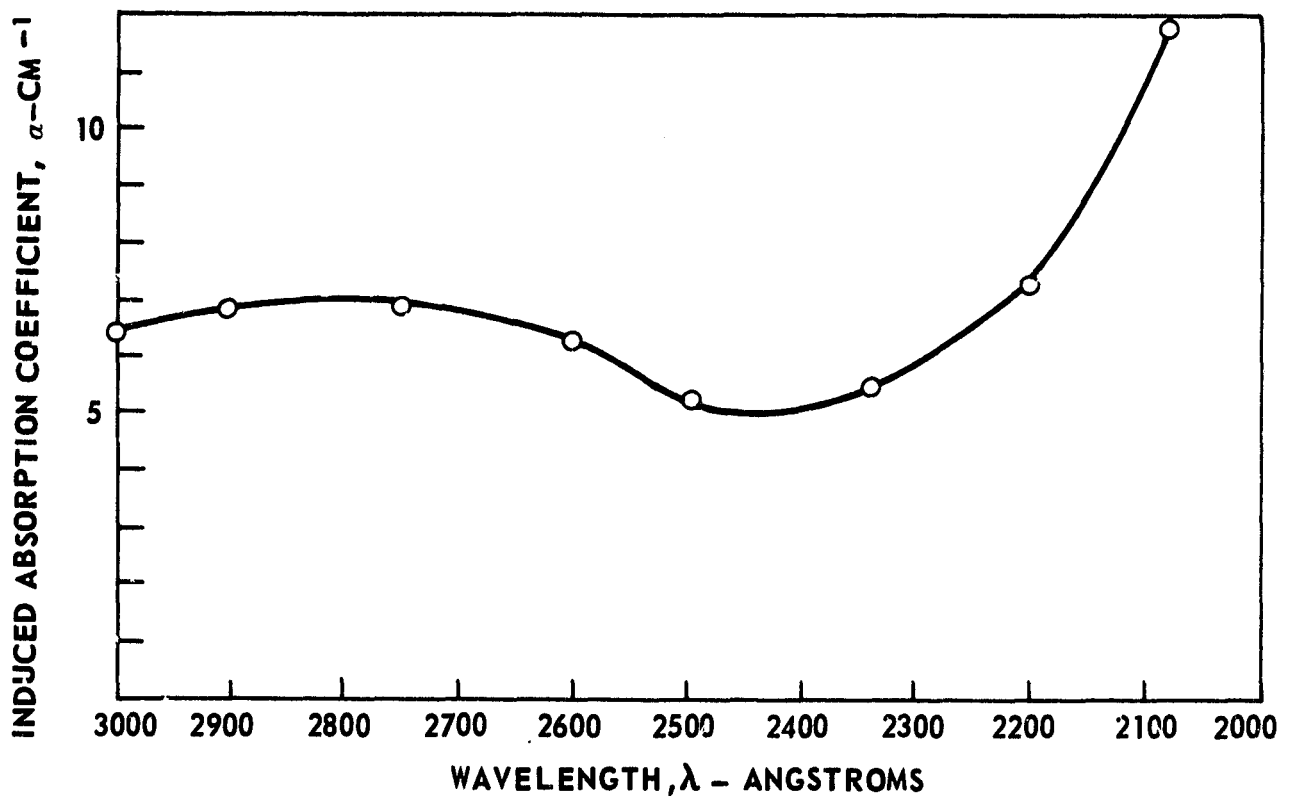
ELAPSED TIME, t - SEC



ABSORPTION SPECTRA OF BARIUM FLOURIDE DURING 1.5 Mev  
ELECTRON IRRADIATION

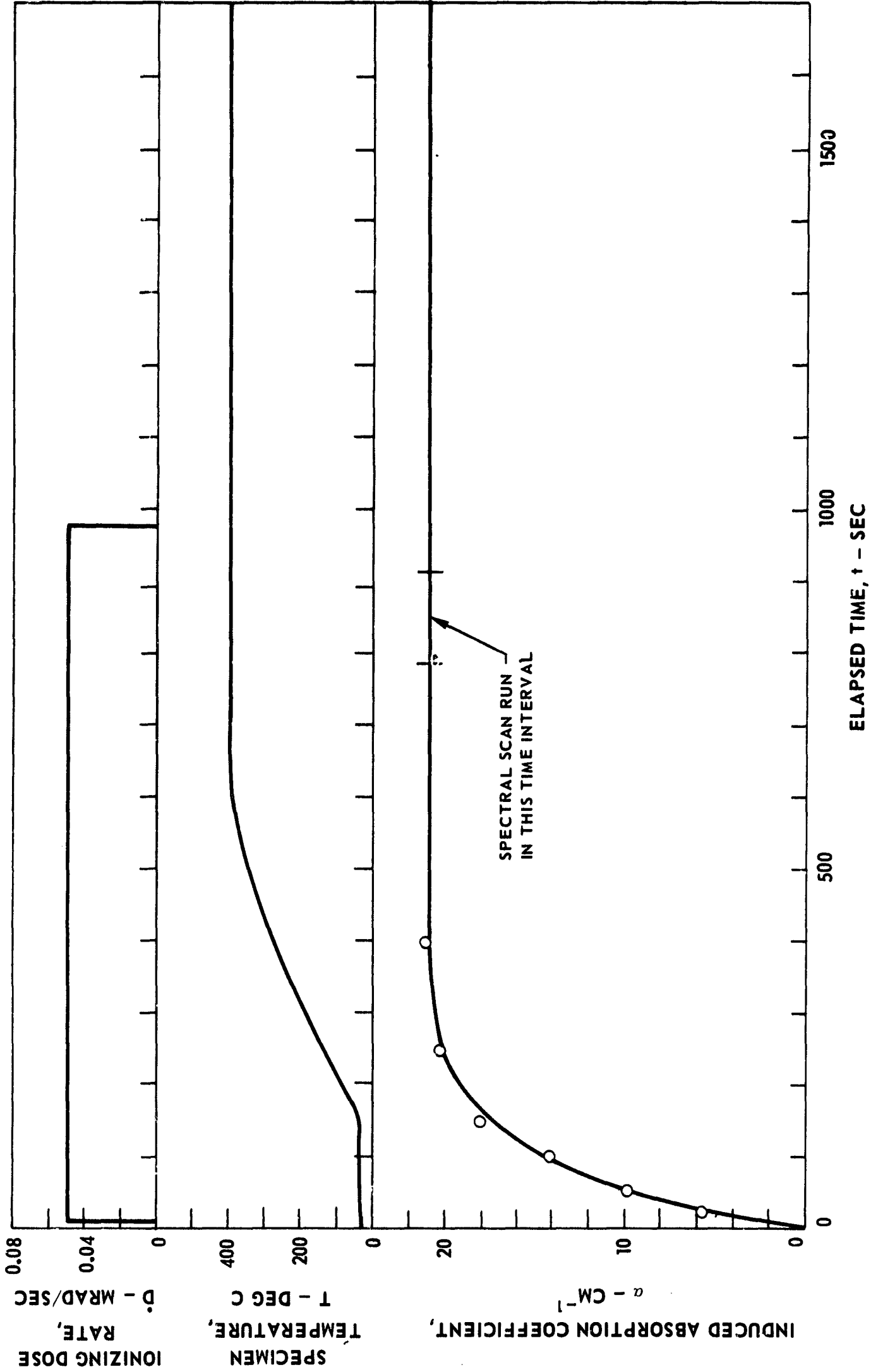
$\dot{D} = 0.65$  MRAD/SEC

T = 70 DEG C



IRADIATION HISTORY OF LIF SPECIMEN

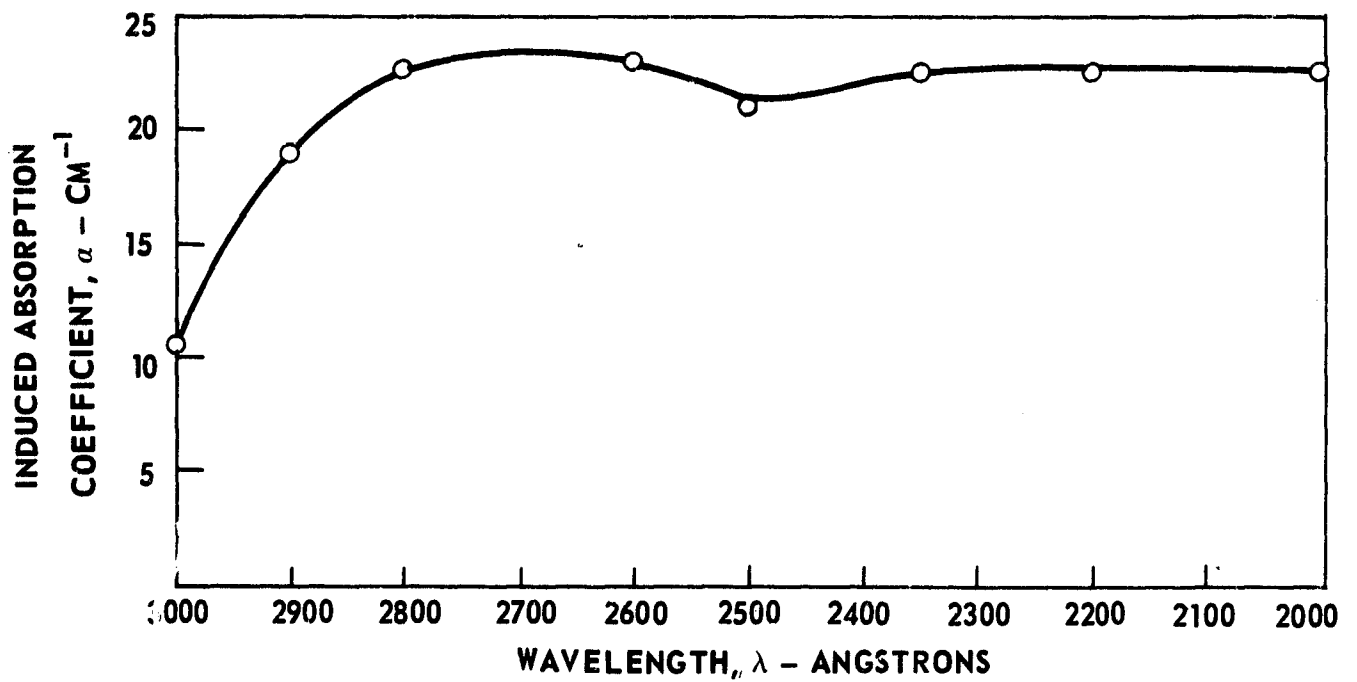
$\lambda = 2500 \text{ \AA}$



ABSORPTION SPECTRA OF LITHIUM FLUORIDE DURING 1.5 Mev  
ELECTRON IRRADIATION

$\dot{D} = 0.05$  MRAD/SEC

T = 400 C



# IRRADIATION HISTORY OF BeO SPECIMEN

$\lambda = 2500 \text{ \AA}$

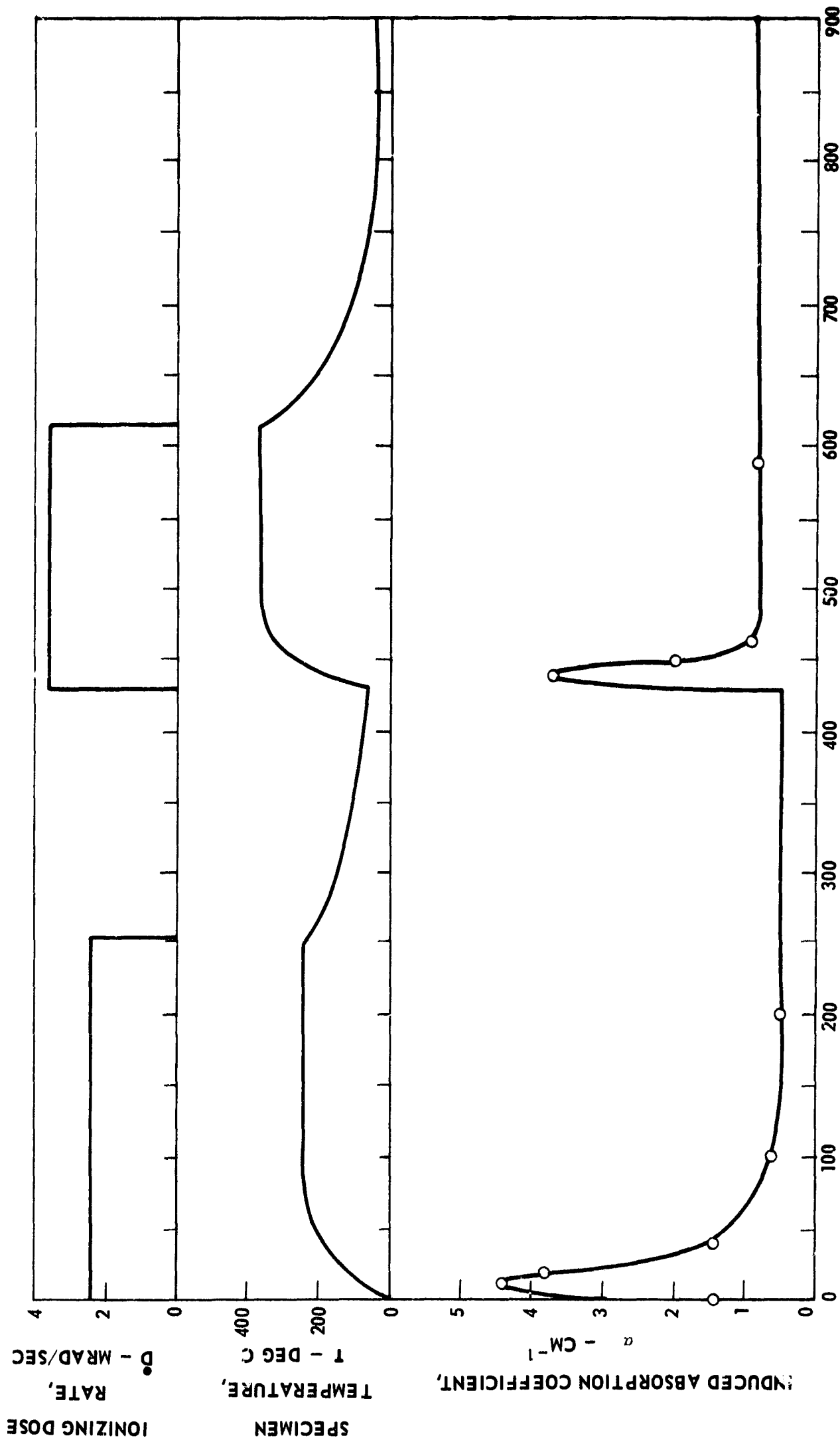


FIG. 24

ELAPSED TIME, t - SEC